THE UNIVERSITY OF CALGARY

Structural Analysis and Epitope Mapping of CD20

by

Maria J. Polyak

A THESIS

SUBMITTED TO THE FACULTY OF GRADUATE STUDIES

IN PARTIAL FULMILLMENT OF THE REQUIREMENTS FOR THE

DEGREE OF MASTER OF SCIENCE

DEPARTMENT OF BIOCHEMISTRY AND MOLECULAR BIOLOGY

CALGARY, ALBERTA

DECEMBER 1, 1999

Abstract

CD20 is a B cell integral membrane protein thought to be involved in B cell activation and antibody production. Evidence for its function has been acquired using antibody ligation of the human CD20 extracellular domain. Cross-blocking experiments have indicated the existence of only two extracellular epitopes, however, additional differences in fine specificity are suggested by the variety of biochemical effects and biological responses induced by various anti-CD20 monoclonal antibodies (mAbs). Despite few differences between human and murine CD20, anti-human CD20 mAbs do not recognize murine epitopes. This would suggest the epitopes are likely comprised of adjacent CD20 molecules. In this thesis, I demonstrated that, contrary to the cross-blocking experiments, there are three extracellular epitopes. These epitopes are on molecules in a ~200 kDa complex primarily comprised of CD20 with a minor ~45 kDa component. Prior to conducting the epitope mapping studies, CD20 membrane orientation was confirmed.

Acknowledgements

I would like to acknowledge my supervisor, Dr. Julie P. Deans, for her leadership, enthusiasm and support as well as Dr. Joe Goren, Dr. John Reynolds and Dr. Steve Robbins for their guidance. In addition, I would like to thank Dr. Chris Brown for his participation in the Thesis Defense as an external examiner. I would also like to thank all the individuals I have had the pleasure of working with during the course of my thesis.

Table of Contents

List of Tables

List of Figures

Abbreviations Used:

Ab, antibody
AARP, IgM Ab-Related Polyneuropathy
BCR, B cell antigen receptor
BSA, bovine serum albumin
Btk, Bruton's tyrosine kinase
C-terminus, carboxy terminus
DAG, diacylglycerol
FACs, fluorescence activated cell sorter
FBS, fetal bovine serum
FcγRIIB, Fc gamma receptor (low affinity)
FcεRI, Fc epsilon receptor (high affinity)
IL, interleukin
IP_3, inositol trisphosphate
ITAM, immunoreceptor tyrosine-based activation motif
ITIM, immunoreceptor tryrosine-based inhibition motif
kDa, kiloDalton
mAb, monclonal antibody
MHCII, major histocompatibility complex class II
m/hCD20, murine/human chimera CD20; human CD20 with a murine extracellular domain
N-terminus, amino terminus
OVA, ovalbumin
P, peptide
PCR, polymerase chain reaction
PBS, phosphate-buffered saline
PI-3K, phosphatidylinositol 3 kinase
PIP_2, phosphatidylinositol-4, 5-diphosphate
PLCγ, phospholipase Cγ
PMA, phorbol-12-myristate-13-acetate
PKC, protein kinase C
SHIP, SH2-containing inositol phophatase
SDS, sodium dodecyl sulfate
SDS-PAGE, SDS polyacrylamide gel electrophoresis
SLE, systemic lupus erythematosus
TM, transmembrane
MW, molecular weight

I. INTRODUCTION

A. An Overview: The Humoral Immune Response

Adaptive immunity can be divided into two components: cell-mediated immunity and humoral immunity. T cells are associated with cell-mediated immunity, while B cells are responsible for the humoral immune response, specifically, the immunity mediated by antibodies (Abs) (1). Bone marrow hematopoeitic stem cells go through a sequence of developmental stages resulting in the formation of several types of cells including immature B cells which express cell-surface immunoglobulin primarily in the form of IgM (1). This cell-surface immunoglobulin comprises the part of the B cell antigen receptor (BCR) which is responsible for recognizing antigen. Before leaving the bone marrow, self-antigen recognizing immature B cells are eliminated via clonal deletion (2).

Those cells which survive negative selection emigrate into the periphery where they scan for antigen. Activation of these mature B cells to produce antibodies occurs via interaction of foreign substances or antigen with the BCR. A cascade of signaling events leads to increased synthesis of proteins and up-regulation of cell surface receptors such as major histocompatibility complex class II (MHCII). These signals culminate in B cell proliferation and differentiation (2).

B cell activation can occur with or without co-stimulation. Some B cells can develop into plasma cells after interacting with antigen without additional signals from activated T helper cells. Antigen which can activate B cells without T cell co-stimulation is known as T-independent antigen. These antigens, such as bacterial polysaccharides and

bacterial toxins, are characterized by their repetitive structure and ability to cause BCR cross-linking which result in high levels of BCR signaling and subsequent secretion of antigen-specific IgM Abs (2).

In most cases, B cell activation requires co-stimulation from T cells. Activation of B cells by monovalent antigen requires co-stimulation from activated T helper cells. These T-dependent antigens do not cross-link the BCR and stimulate a lower degree of BCR signaling. Upon ligation, the BCR-antigen complex is internalized. The antigen is processed and presented in context of MHCII on the surface of B cells. The antigen:MHCII complex is recognized by the T cell antigen receptor on T helper cells which then become activated. This results in the up-regulation of the T cell CD40 ligand and the secretion of B cell stimulatory cytokines, including interleukin 4 (IL-4), IL-5 and IL-6. B cells are co-stimulated by IL-4 and interaction of CD40 ligand with the B cell integral membrane protein CD40 (2). Co-stimulation results in B cell secretion of primary IgM and IgG antibody with low affinity for antigen. Isotype switching from IgM to IgG initiates B cell affinity maturation (3).

Spleen and lymph node germinal centers are the site of activated B cell affinity maturation. Germinal centers form as a result of antigen recognition and are comprised of activated B cells, activated T helper cells and antigen-presenting follicular dendritic cells (3-5).

There are two stages of affinity maturation: proliferation and affinity selection (6). In the presence of T cell help, activated B cells undergo extensive somatic hypermutation and proliferation which is known as clonal expansion (4, 6). As a result, a single B cell

can expand into a population of B cells having varied affinities for antigen. These B cells then come into contact with immune complexes comprised of antigen, complement and primary Ab localized on follicular dendritic cells (FDCs) (3). Once B cells interact with these immune complexes, there is enhanced presentation of antigen in context of MHCII and secretion of the cytokines IL-4, IL-5 and IL-10 by activated T cells (7). Those B cells having greatest affinity for antigen then undergo isotype switching and differentiate into memory cells and antibody-secreting plasma cells (5). The differentiation pathway taken by the cells depends on the signals present. In vitro, memory B cells are generated in the presence of CD40 ligand, IL-2 and IL-10, while plasma cells form in the presence of IL-2 and IL-10 (8). The remaining majority of B cells die (4).

Not all self-reactive B cells are removed in the bone marrow. Some mature B cells recognize self-antigen in the periphery. Several mechanisms exist to deal with these cells. Self reactive cells are either eliminated or inactivated by contact with self antigen (2). Failure of these processes can result in an immune response against self (2). Chronic production of self-directed antibodies are manifested as autoimmune diseases including systemic lupus erythematosus (SLE) (9, 10).

B. B Cell Antigen Receptor Complex and its Activation

The BCR complex is comprised of a membrane-bound immunoglobulin which is non-covalently associated with the disulfide linked Igα and Igβ chains. The membrane-

bound immunoglobulin recognizes antigen, while the Igα and Igβ chains are required for cell-surface immunoglobulin, specifically IgM, expression and signal transduction (1).

The cytoplasmic domains of the Igα and Igβ chains contain a sequence of highly conserved amino acids ($YXXL(X_{6-7})YXXL$) called immunoreceptor tyrosine-based activation motifs (ITAM) (11). Upon BCR ligation with antigen, the src-family tyrosine kinases, blk, lck, fyn, and lyn are activated resulting in the phosphorylation of the four ITAM tryrosines and subsequent recruitment of syk (12, 13).

As a result, three intracellular signaling pathways are initiated (12, 14). Activated syk in conjunction with Bruton's tyrosine kinase (Btk), which is also activated after BCR ligation by the src family kinases, phosphorylate and activate phospholipase C γ (PLCγ) (15). PLCγ then hydrolyzes PIP_2 into inositol trisphosphate (IP_3) and diacylglycerol (DAG) resulting in release of calcium from intracellular stores and activation of protein kinase C (PKC) (12, 16). BCR activation activates the MAP kinase pathway via tyrosine phosphorylation of vav as well as by initiation of the Ras pathway (17, 18). Phosphotidylinositol-3-kinase (PI-3K) is also activated upon BCR ligation in a protein tyrosine kinase-dependent fashion (1, 19, 12, 20).

The recently identified protein BLNK/SLP-65 has also been shown to be rapidly tyrosine phosphorylated upon BCR activation. Once it is phosphorylated, BLNK/SLP-65 can bind PLCγ and vav (21). The observation that it can translocate from the cytosol to the plasma membrane suggests it may act as an adaptor for bringing downstream effectors into closer proximity to syk (14, 22).

As a result of the activation of these signal transduction pathways, several molecular and biochemical changes occur which include antigen presentation, gene transcription, proliferation and immunoglobulin secretion.

C. Modulation of BCR Activation

The threshold of B cell activation is modulated by a variety of cell surface co-receptors and soluble factors. The B cell modulators include the CD19 co-receptor complex, CD22, and FcγRIIB1 as well as cytokines. The cytokines such as IL-2, IL-4 and IL-13 have been shown to promote B cell proliferation. The cytokines IL-4 and IL-13 secreted by T cells are able to promote human, but not mouse, B cell proliferation, and activation and immunoglobulin heavy-chain switching upon binding their receptors on B cells (23).

1. The CD19 Co-receptor Complex

The CD19 co-receptor is comprised of four components: Leu-13, CD81 (TAPA-1), the complement receptor CD21 and CD19 (24, 25). CD19 acts to lower the threshold of B cell activation via its constitutive association with the BCR (26). This is achieved by enhancing the calcium response and phosphorylation of src family kinases induced by BCR signaling (27). Although co-ligation of the CD19 co-receptor complex and BCR is not required for signal enhancement, cross-linking this co-receptor with BCR amplifies the response of BCR to antigen even further (28, 25, 29). Upon the binding of

C3d complement complexed with antigen to CD21, the CD19 co-receptor complex association with the BCR is enhanced (25, 30). This association leads to the tyrosine phosphorylation of CD19 and subsequent recruitment of PI3-K (28) and src-family kinases including lyn (29, 31) and vav (25, 30, 32). Studies on CD19 deficient mice have shown CD19 to be important in germinal center formation and affinity maturation (33).

2. Down-regulation of the B Cell Response

2.1 CD22

CD22 is a cell surface adhesion molecule which has been shown to constitutively down-regulate BCR signaling. CD22 can bind a variety of glycoproteins and glycolipids, including CD45RO on T cells, indicating that binding its ligand may facilitate B cell activation (34). The src family kinase lyn which is involved in the BCR activation signal also acts in the CD22 inhibitory pathway (24). Upon BCR cross-linking, CD22 intracytoplasmic tyrosines within immunoreceptor tyrosine-based inhibition motifs (ITIM) are phosphorylated by lyn and the phosphatase SHP-1 is recruited. Cross-linking of CD22 with either BCR or BCR and CD19 causes the suppression of the MAP kinase pathway (35), which is a pathway responsible for gene expression. In CD22 deficient mice, splenic B cells were found to be hyperresponsive to BCR cross-linking and there were higher levels of serum IgM and autoantibodies (36). These results are very similar to those observed in lyn deficient mice (37, 38) as well as in motheaten mice which are SHP-1 deficient (39, 40). Recently, data acquired using CD19/CD22-deficient and

CD19-deficient mice suggests that CD19 is necessary for initation of the CD22 inhibitory pathway and CD22 then acts by down-regulating CD19 (41).

2.2 FcγRIIB1

FcγRIIB1 down-regulates the immune response in B cells. Unlike the BCR which binds only specific antigen, FcγRIIB1 binds any antigen within an IgG immune complex. Simultaneous signaling through the BCR by antigen and FcγRIIB1 by antibody in mature B cells inhibits BCR activation (42). This prevents mature B cells from responding to an antigen against which the body has already mounted an immune response. As well, since co-ligation of BCR with FcγRIIB1 prevents its internalization, FcγRIIB1 prevents processing of bound antigen and subsequent T cell activation (43).

Cross-linking of the BCR and FcγRIIB1 results in aggregation of these receptors in cap structures on the plasma membrane. The redistribution of FcγRIIB1 to caps with the BCR as well as other molecules involved in the activation process such as MHCII, CD19 and H-ras may ensure that the receptor is in close proximity to those molecules which it may regulate (44).

Co-ligation of the BCR and FcgRIIB1 initiates a series of signaling events culminating with termination of activation signals. FcγRIIB1 inhibitory signals are initiated by the phosphorylation of its intracytoplasmic ITIM (45, 46) by lyn (45). The inositol phosphatase SHIP is then recruited (47). Eventually, BCR activation signals are directly countered by the reduction of PLCγ phosphorylation (48), thereby, diminishing

IP_3 generation (46) and calcium influx (16, 44, 46). Concomitantly, there is a reduction in CD19 phosphorylation (49, 50) and gene transcription (51) as well as inhibition of the ras pathway (52). The end result is the inhibition of B cell proliferation (16, 46, 53), immunoglobulin secretion (24), and internalization of antigen (43). Although engagement of FcγRIIB1 has been shown to result in cell death, it was recently shown that this process is SHIP independent (54).

D. Modulation of the B Cell Response by CD20

1. CD20 Overview

The B cell specific integral membrane phosphoprotein CD20 (33/35 kDa) is also thought to be a modulator of B cell development, activation and differentiation. It has been shown to be physically and functionally associated with MHCII (55, 56) and CD40 (57, 56, 58). CD20 is expressed from the pre-B cell to the mature B cell stage of development, but is not present on plasma cells (59). The precise role of CD20 is not known. It may act as a receptor, a signaling component of a receptor complex or even a calcium channel (60).

2. Evidence for CD20 Function

Evidence for the role of CD20 in B cell development and activation has primarily come from *in vitro* studies using anti-CD20 monoclonal antibodies (mAbs). The anti-CD20 mAbs have several different effects on B cells depending upon the stage of B cell

differentiation. 1F5 anti-CD20 mAb induces G0/G1 transition (61-64) characterised by the up-regulation of MHC II (62, 65) and the oncogenes c-myc (64, 65) and B-myb (57). 1F5 stimulation alone is not sufficient for transition into the S and G2+M phases of the cell cycle and subsequent B cell proliferation (63). Additional stimulation with anti-CD40 mAb is required for B cell proliferation. CD20 and CD40 co-stimulation is characterised by the up-regulation of the three oncogenes c-myc, B-myb, and c-myb (57) which are also induced during mitogenic stimulation of B cells.

CD40 also seems to have a role in maintaining the conformation of CD20. Anti-CD40 mAb reverses the effects of IL-4 on CD20. IL-4 down-regulates the epitope recognized by the anti-CD20 antibody L27 possibly as a result of a conformational change in CD20 (58). Both CD40 and IL-4 have important roles in the proliferation of activated B cells. Maintenance of CD20 conformation may be important in B cell proliferation.

Unlike 1F5, most anti-CD20 mAbs inhibit B cell activation. The B1 anti-CD20 mAb, which has the same IgG2a isotype and same specificity for CD20 as 1F5, does not activate B cells (63). Although 1F5 binding to CD20 can activate B cells, both 1F5 and B1 mAbs inhibit mitogen stimulated B cell cycle progression and differentiation into immunoglobulin secreting cells (63, 66). B1 mAb has been shown to inhibit differentiation and immunoglobulin secretion of pokeweed mitogen (66), Epstein-Barr virus (67, 68) or staphylococcus aureus Cowan I-induced (68) B cells, while it has little effect on anti-μ activated B cells. Although B1 inhibits B cell cycle progression, B1

interaction with CD20 does not affect early activation events (66, 67). Another effect of B1 binding to CD20, is the up-regulation of CD18 and a yet unidentified adhesion molecule resulting in B cell homotypic adhesion (69). The different effects observed with B1 compared to 1F5 may be the result from the overlapping or possibly different CD20 epitopes recognized by the two mAbs as has been suggested by cross-blocking studies (70).

Like B1, the anti-CD20 mAb 2H7 also does not activate B cells (61). 2H7 has an isotype of IgG2b, different than that of 1F5 and B1, but cross-blocking studies have suggested it recognizes the same epitope as B1 (70). Despite this, 2H7 and B1 differ markedly in their ability to co-precipitate CD20-associated molecules (71) and to induce redistribution of CD20 to detergent-insoluble microdomains (72).

2.1 Immunotherapy

The first antibody approved for chemotherapy, Rituxan™, is against CD20. This humanized mouse mAb has been demonstrated to be efficacious against the B cell mediated cancer non-Hodgkins lymphoma (73) as well as the autoimmune disease, IgM Ab-Related Polyneuropathies (AARP's) (74). In those patients being treated for non-Hodgkins lymphoma, ~50% have gone into remission of approximately one year in duration (73). All AARP patients treated showed improved function as reflected by increased strength as well as reduced serum autoantibody titres (74). It is thought that Rituxan™ acts by eliminating B cells via complement-mediated lysis, antibody-dependent cell mediated cytotoxicity, and primarily by signaling through CD20 leading to apoptosis (73, 75).

2.2 Apoptosis

Indeed, *in vitro* studies examining the mechanism of action of this immunotherapy has demonstrated that extensive cross-linking of anti-CD20 mAbs using either goat anti-mouse IgG or FcR-expressing cells directly inhibits B cell proliferation and leads to cell death by apoptosis (75). Hyper-cross-linking of the mAbs 1F5, 2H7 and B1 resulted in B cell apoptosis via signaling events leading to increased intracellular calcium levels (75). This suggested that the depletion of malignant or autoreactive B cells by Rituxan™ was the direct result of signals induced upon CD20 ligation leading to apoptosis. *In vivo*, however, immune complexes formed by therapeutic mAbs may be retained by follicular dendritic cells in the germinal center and cross-link B cell FcγRIIB resulting in SHIP-independent apoptosis (54).

3. CD20 Signaling

The effects of the anti-CD20 mAbs on B cells indicate that stimulation through CD20 results in signal transduction. There is some further evidence indicating that it plays a role in signal transduction. CD20 is not glycosylated, but is differentially phosphorylated at intracellular serine and threonine residues (76). Mitogen stimulation of B cells results in increased expression and phosphorylation of CD20 (76). In vitro assays indicate that several kinases are capable of phosphorylating CD20 at unique residues which may result in different functional consequences under physiological conditions (60). Antibody ligation of CD20 also induces the phosphorylation of cellular proteins on

serine/threonine and tyrosine residues (71). CD20 is associated with the tyrosine kinases lyn, fyn and lck and the yet unidentified p75/80 (71).

4. CD20 Sequence

CD20 is related to two four transmembrane domain containing proteins, the β subunit of the high-affinity receptor for IgE, FcεRIβ (77) and the hematopoietic protein HTm4 (78). The genes of each member of this four transmembrane protein family map to human chromosome 11 (68, 78), while the genes of CD20 and FcεRIβ map to murine chromosome 19 (78, 79). These proteins are about 20% homologous with the greatest degree of homology occurring in the transmembrane domains. FcεRIβ is one of the signal transduction components of the high affinity IgE receptor, FcεRI serving to amplify signals (80, 81). Like FcεRIβ, CD20 has a role in signal transduction and may be a component in a yet unidentified receptor complex.

Human CD20 and its murine counterpart, Ly-44, have been cloned and their genetic sequences characterized (79, 82, 83). The coding region of the human CD20 cDNA shares an 82% sequence homology with the murine nucleotide sequence. Protein sequences have been derived from these nucleotide sequences. At the amino acid level, there is 73% homology between the human and murine sequences with most of the differences arising from conservative substitutions.

Based on hydrophobicity data and a lack of a signal sequence, the membrane topology of both human and murine CD20 have been proposed (79, 83), but have not

been confirmed experimentally. The proposed orientation of the CD20 homologs may be incorrect since signal sequences are not always necessary for extracellular localization of N-terminal regions (84-89). Both CD20 homologs are presumed to have intracellular N- and C-terminal domains, four transmembrane domains and extracellular loops potentially between the first and second as well as the third and fourth transmembrane domains (79, 83). Four cysteines are conserved between the homologs (79, 83). The two which are present in the proposed extracellular domain may form a disulfide bond (79).

The human and murine CD20 transmembrane and cytoplasmic regions are highly homologous. The predicted extracellular regions are the least conserved having 66% homology (79). Sixteen of the forty four amino acid residues in the extracellular domain are non-homologous. Of these, only eight are non-conservative substitutions yet the anti-human CD20 mAbs do not recognize the murine form of CD20 (70).

CD20 ligation can result in its rapid redistribution to detergent-insoluble microdomains otherwise known as lipid rafts (72). The degree of redistribution is dependent upon the ligating mAb (72). CD20 redistribution is dependent upon the membrane proximal residues 219-252 in the cytoplasmic C-terminal domain (90). This stretch of membrane proximal C-terminal residues includes a cysteine residue at position 220 that is conserved in the other two members of the CD20 family of related proteins, i.e., FcεRIβ and HTm4 (78, 91). The proximity of Cys220 to the inner leaflet of the plasma membrane makes it a potential site of reversible lipid modification by palmitoyl transferase. Palmitoylation is required for the caveolar localization of the Src family

tyrosine kinase Hck and the endothelial nitric oxide synthase (92, 93), and is found on a number of other proteins in these microdomains, including several of the Gα signaling proteins and caveolin, a structural protein of caveolae. However, mutation of Cys220 did not affect redistribution to lipid rafts. Although not required for CD20 redistribution, this cysteine residue may still be palmitoylated. Similarly, caveolin is palmitoylated, but this modification is not required for caveolar localization of caveolin (94).

5. The Calcium Channel

Its structure and homooligomeric nature in conjunction with its ability to conduct calcium has made some investigators postulate that CD20 is a voltage independent calcium channel. Chemical cross-linking studies indicate that CD20 exists as a monomer, dimer and tetramer (95). Other well characterized ion channels including the rat brain sodium channel (96) and $GABA_a$ receptor chloride channel (97) span the membrane four times and are homooligomeric (83, 95).

The evidence for CD20 as a calcium channel is controversial. CD20 mediated current has been observed using whole cell patch clamp analysis of membrane conductance in both a B cell lineage as well as in cells ectopically expressing CD20 (95, 98, 99). In at least two of the studies (95, 98), the current observed is very small and the contribution of ions other than calcium cannot be excluded (personal communication of Dr. Deans with Dr. Deutsch). Other investigators have not been able to observe a CD20 induced calcium current. A calcium current could not be observed with either stimulation

of CD20 or depletion of intracellular calcium in both a B cell line and a CD20 transfected cell line as monitored using whole cell patch clamp analysis (personal communication of Dr. Deans with Dr. Deutsch; 100). However, there does appear to be a small current attributable to calcium in a CD20 transfected cell line compared to control which cannot be dismissed in one study (personal communication of Dr. Deans with Dr. Deutsch; 98).

Intracellular calcium levels monitored using fluorescence microscopy indicated increased plasma membrane calcium permeability in CD20 transfected cells as compared to controls (95). As well, 1F5 ligation of CD20 on a B cell line caused an acute change in the calcium current as observed using whole cell patch clamp (95), but not with fluorescence measurements (95, 101). B1 binding to CD20 on spleen B cells had no acute affect on intracellular calcium (66), but had an affect on intracellular calcium levels on a B cell line after 24 hrs treatment (95). Fluorescence studies demonstrated calcium flux at least part from intracellular stores after treating Ramos B cells and normal peripheral blood B cells with cross-linked anti-CD20 mAb. Both 2H7 and 1F5 increased intracellular calcium although the response was slightly weaker for 1F5 (102).

Based on these results, CD20 may or may not be a calcium channel. However, the results do indicate that CD20 enhances current activity and affects intracellular calcium. There are several possibilities for its role including 1) CD20 is a calcium channel, 2) CD20 is associated with a channel thereby regulating calcium flux via an adjacent channel, or 3) CD20 stimulation initiates signals which modulate a calcium channel.

E. Significance

CD20 is a B cell integral membrane protein thought to regulate intracellular calcium and to be involved in B cell activation and control of antibody production. Evidence for its function has been acquired using antibody ligation of the extracellular domain of human CD20. Cross-blocking experiments have indicated the existence of only two overlapping extracellular epitopes, however, additional differences in fine specificity are suggested by the variety of biochemical effects and biological responses induced by various anti-CD20 monoclonal antibodies (mAbs) (Table I.1). The variety of responses induced by the anti-CD20 mAbs are likely a result of unique conformational shifts in the protein induced upon ligation with subsequent changes in protein association and downstream signaling events. Understanding these differences and their consequences may aid in identifying the specific role of CD20 in the B cell and, in turn, in the humoral immune response.

Table I.1. Summary of Biochemical Effects and Biological Responses Induced by Different Anti-CD20 mAbs (NT = not tested)

	Anti-CD20 mAb		
	1F5	**2H7**	**B1**
Activates resting B cells	++++	-	-
Blocks terminal differentiation	++++	++++	++++
Induces B cell aggregation	-	-	++++
Induces CD20 redistribution	++	++++	+
Precipitates CD20 from lysate	+/-	+/-	+++
Co-precipitates p75/80	+	++++	+
Co-precipitates kinase activity	+	++++	+
Induces calcium flux (cross-linked)	-	++	NT
Induces B cell apoptosis (cross-linked)	++++	++++	++++

F. Hypothesis

The various anti-CD20 mAbs recognize unique discontinuous epitopes on adjacent molecules in the CD20 complex.

G. Objectives:

1. Structural Analysis

1.1 Membrane Orientation: To confirm the membrane orientation of CD20

1.2 CD20 Complex: To confirm the size of the CD20 complex

2. Epitope Mapping

a) To determine whether the epitopes recognized by a panel of anti-CD20 mAbs are linear or discontinuous

b) To identify the amino acid residues which comprise the epitopes of a panel of anti-CD20 mAbs

II. MATERIALS AND METHODS

The following describes the various materials and methods which were used to address the objectives of my hypothesis.

A. Cells and Antibodies

Several cell lines and antibodies were utilized throughout my experiments. Raji lymphoblastoid B cells were grown in RPMI/5% fetal bovine serum (FBS). Molt-4 T cells expressing stably transfected CD20 N- and C-terminal deletion mutants previously established in our laboratory were grown in RPMI/10%FBS, with 0.4 mg/ml geneticin (Life Technologies, Gaithersburg, MD). HEK 293 cells used for transient transfection were grown in DMEM/10% FBS.

1F5 (IgG2a), 2H7 (IgG2b) and B1 (IgG2a) CD20-specific mAbs were used with the appropriate isotype controls. 1F5 and 2H7 mAb were provided by Dr. J. Ledbetter (Bristol-Myers Squibb, Seattle, WA). B1 mAb was purchased from Coulter. Antisera against the amino and carboxyl regions of CD20 (herein named anti-CD20N and anti-CD20C) were generated by immunizing rabbits with either ovalbumin (OVA) -conjugated CD20N peptide (CD20N-P; residues 25-41, SGPKPLFRRMSSLVGPT) or OVA-conjugated CD20C peptide (CD20C-P; residues 231-245, SAEEKKEQTIEIKEE; peptides were provided by James Blake, Bristol-Myers Squibb). The Abs were affinity purified using the Pierce Sulfolink Kit (Rockford, IL) and used for immunofluorescence, immunoprecipitation and immunoblotting. Antisera against another carboxyl terminal

peptide (referred to as anti-CD20C2) was generated in our laboratory against GST-conjugated CD20C2 peptide (CD20C2; residues 280-297, PEPPZDQESSPIENDSSP) and used for immunoblotting. In the velocity gradient experiments, PLCγ mAb (Transduction Laboratories, Lexington, KY) and anti-gp130 Ab provided by Dr. Steve Robbins (University of Calgary, Calgary, Canada) were used for controls.

B. Mutagenesis and Transfections

Several CD20 truncation mutants and extracellular domain mutants were utilized in various experiments.

1. Cytoplasmic Deletion Mutants

The cytoplasmic deletion mutants in which residues 1-49, 219-252 or 253-297 were removed (referred to as NΔ1-49, CΔ219-252 and CΔ253-297) were developed previously in our laboratory (71, 90).

2. Extracellular Domain Mutants

Extracellular domain mutants for the epitope mapping studies were generated using overlap extension PCR using internal primer pairs (Tables 3 and 4) and either human CD20 cDNA template (to generate CD20 Mutants 1-7), Mutant 7 cDNA template (to generate human CD20 with a murine extracellular domain, referred to as m/hCD20, and Mutants A and C) or m/hCD20 template (to generate Mutants B and D).

Outside primers used were 5'-ATAATGAATTCATTGAGCCTCTTT-3' (5' primer that includes a unique EcoRI restriction site at position 451 of the CD20 cDNA) and 5'-AATCACTTAAGGAGAGCT-3' (3' primer that includes a unique AflII site at position 983).

For the negative binding studies, the extracellular domain of human CD20 was converted stepwise toward murine (Mutants 1-7) using the internal primer pairs shown in Table II.1. For the positive binding studies, the human extracellular domain was converted to murine using the internal primer pairs listed and then the murine sequence was systematically humanized (Mutants A-D) using the internal primer pairs shown in Table II.2. The PCR fragments were digested with EcoRI and AflII, then cloned into pBluescript containing human CD20 cDNA insert from which the EcoRI/AflII fragment had been excised. The sequence of each construct was confirmed prior to subcloning into the XhoI/NotI site of the pCDM8 mammalian expression vector.

3. Transient Transfection of Extracellular Domain Mutant cDNA

HEK 293 cells grown to ~50% confluence in 10 cm tissue culture plates (Falcon) were transiently transfected with CD20 extracellular domain wild type and mutant constructs by the calcium phosphate method. 20 μg DNA was brought up to 450 μl final volume with sterile dd$H_2$0. 50 μl 2.5 M $CaCl_2$ was added to the diluted DNA to a final concentration of 250 mM. The DNA-$CaCl_2$ mixture was then slowly bubbled into an

Table II.1. Extracellular Domain Mutants used in the Negative Binding Strategy: Internal Primer Pairs Converting Human CD20 Extracellular Domain to Murine

Mutant	Forward 5' Primer	Reverse 3' Primer
Mutant 1 (KI/TL)	5'-CTT AAT ATT ACA CTT TCC CAT-3'	5'-A ATG GGA AAAG TGT AAT ATT AAG-3'
Mutant 2 (ES/RR)	5'-TTA AAG ATG AGG AGA CTG AAT TT-3'	5'-AA ATT CAG TCT CCT CAT CTT TAA-3'
Mutant 3 (NF/EL)	5'-GAG AGT CTG GAG CTT ATT AGA G-3'	C TCT AAT AAG CTC CAG ACT CTC-3'
Mutant 4 (RAHT/QTSK)	5'-G AAT TTC ATT CAA ACT TCC AAA CCA TAT ATT-3'	5'-AAT ATA TGG TTT GGA AGT TTG AAT GAA ATT C-3'
Mutant 5 (INIYN/VDIYD)	5'-CA CCA TAT GTT GAC ATA TAC GAC TGT GAA CC-3'	5'-GG TTC ACA GTC GTA TAT GTC AAC ATA TGG TG-3'
Mutant 6 (ANP/SNS)	5'-GT GAA CCA TCT AAT TCC TCT GAG-3'	5'-CTC AGA GGA ATT AGA TGG TTC AC-3'
Mutant 7 (Y/N)	5'-C CAA TAC TGT AAC AGC ATA C-3'	5'-G TAT GCT GTT ACA GTA TTG G-3'

Table II.2. Extracellular Domain Mutants used in the Positive Binding Strategy: Internal Primer Pairs Converting entire Human CD20 Extracellular Domain to Murine and Converting m/hCD20 Stepwise Toward Human

Mutant	Forward 5' Primer	Reverse 3' Primer
m/hCD20	5'-TA AA ATG AGG AGA CTG GAG CTT ATT CAA ACT TCC AAA CCA TAT GTT GAC ATC TAC GAC TGT GAA CCA TCT AAT TCC TCT GAG-3'	5'-ATA TGG TTT GGA AGT TTG AAT AAG CTC CAG TCT CCT CAT TTT TAA AAA ATG AGA AAG TGT AAT ATT AAG-3'
A	5'-A CCA TAT GTT GAC ATC TAC GAC TGT GAA CCA TCT AAT TCC TCT GAG-3'	5'-CTC AGA GGA ATT AGA TGG TTC ACA GTC GTA GAT GTC AAC ATA CGG T-3'
B	5'-CA TAT ATT AAC ATC TAC AAC TG-3'	5'-CA GTT GTA GAT GTT AAT ATA TG-3'
C	5'-TA AAA ATG AGG AGA CTG GAG CTT ATT CAA ACT TCC AAA CCA TAT GTT GAC ATC TAC GAC TGT GAA C-3'	Same as for murine/human CD20
D	5'-CA TCT AAT CCC TCT GAG-3'	5'-CTC AGA GGG ATT AGA TG-3'

equal volume of 500 µl 2X HEPES buffer (280 mM NaCl, 50 mM HEPES, 1.5 mM Na_2HPO_4) and left for no more than 5 min to precipitate before transferring to a HEK 293 culture plate. Two to three days post-transfection, cells were washed 2X with phosphate-buffered saline (PBS; 140 mM NaCl, 2.5 mM KCl, 10 mM Na_2HPO_4, 2 mM KH_2PO_4), lifted off the culture plates and, in most cases, divided for analysis of construct expression by western blot analysis and of antibody binding by FACs analysis.

For the negative binding strategy, Ab binding values were normalized for expression. One-third of cells of each transfectant were lysed in 0.5% Triton X-100 including inhibitors described in Sample Preparation. Total protein concentration of each sample was determined by modified Lowry method using a Biorad Protein assay Kit. Equal amounts of protein were separated by SDS-PAGE and analysed by anti-CD20N immunoblot. Equal protein loading was confirmed by Coomassie stain. Densitometry was performed on CD20 bands and used for normalization of median fluorescence values obtained by FACs analysis of the same transfected cells.

Antibody binding as measured by median fluorescence was normalized to expression as follows.

Net median fluorescence = [Total median flurorescence (anti-CD20 mAb)] - [Total median fluorescence (isotype mAb)]

Ratio of mutant CD20 construct expressed compared to wild type:

$$\text{Ratio} = \frac{[\text{relative density (mutant)}]}{[\text{relative density (wild type)}]}$$

Fluorescence adjusted for CD20 construct expression:

$$\text{Adjusted median fluorescence} = \text{net median fluorescence} \times \frac{1}{\frac{[\text{relative density (mutant)}]}{[\text{relative density (wild type)}]}}$$

To normalize binding to mutant CD20 construct with binding to wild type set at 100:

$$\text{Normal median fluorescence} = \frac{[\text{adjusted median fluorescence}]}{[\text{wild type net median fluorescence}]} \times 100$$

For the positive binding strategy, cell surface expression of constructs was confirmed using proteinase K digest of intact cells and subsequent western blot analysis as described later.

C. Immunofluorescence

Cells were suspended and incubated in RPMI/5% FBS or PBS/2% FBS with anti-CD20 or control Abs, washed once, and resuspended in 100 µl (1/100) dilution of either FITC-conjugated rabbit anti-mouse IgG (Southern Biotechnology Associates, Birmingham, AL) or FITC-conjugated goat anti-rabbit IgG (ICN, Costa Mesa, CA) as appropriate. As a component of the epitope mapping studies, 1F5, 2H7 and B1 mAbs were preincubated with a vast excess of peptide containing a stretch of the least conserved amino acids in the extracellular domain (residues 142-151; ESLNFIRAHT) for 30 min at 37°C. For intracellular staining, Raji B cells (1 X 10^6 cells/sample) were permeabilized with 0.05% saponin in RPMI/5% FBS for 30 min on ice. Subsequent Ab incubation and wash steps were performed as described above, except in the presence of 0.01% saponin. For the peptide inhibition studies, anti-CD20N and anti-CD20C Abs

were preincubated with the immunizing peptides CD20N-P and CD20C-P, respectively, for 3 h at room temperature. Immunofluorescence of all samples was measured using a FACScan cytometer (Becton Dickinson, Mountain View, CA).

D. Trypsin and Proteinase K Digests

To confirm CD20 membrane orientation, trypsin and proteinase K digests were performed on intact Raji cells. Proteinase K digests were also used to confirm cell surface expression of mutants transiently expressed in HEK 293 cells. Raji cells (2 X 10^6 /sample) were washed and resuspended in 50 mM Tris-HCl (pH 7.5), then incubated alone or with trypsin (0.2 μg/μl) for 15 min on ice. For proteinase K digests, cells were washed and resuspended in PBS, then incubated alone or with 12.5 μM Proteinase K for 15 min on ice. Protease inhibitors (4mM Pefabloc (Boehringer Mannheim, Laval, Quebec), 1μg/ml aprotinin, 1μg/ml leupeptin, and 1 mM PMSF) were added to halt digestion. Samples were then rapidly centrifuged, and the supernatants were aspirated. Cell pellets were lysed directly in 2X sample buffer, heated to 100°C for 5 min, and loaded on 12.5% polyacrylamide gels (4 X 10^5 cell equivalents/lane).

E. Sample Preparation

Cells were washed, pelleted and lysed on ice for 15 min in either 0.5% Triton X-100 lysis buffer (immunoprecipitation and transient transfection) or 1% Triton X-100 (sucrose density gradient) or 1% digitonin/MBS (sucrose density gradient; MBS; 150

mM NaCl, 25 mM MES (pH 6.5)) containing protease inhibitors (1μg/ml aprotinin, 1μg/ml leupeptin, 1mM $NaMoO_4$, 1mM $NaVO_4$, 1mM PMSF, 1mM EDTA). Because CD20 can form higher order oligomers via reactive cysteine residues under non-reducing conditions, 100 mM iodoacetamide was also included in the velocity gradient experiments using digitonin to prevent non-specific post-lysis difsulfide bond formation. EDTA was omitted in the sucrose density gradient experiments while 2mM $CaCl_2$ was added since EDTA chelates divalent cations which could be required for stabilizing the CD20 complex. Samples were centrifuged to pellet the insoluble material. The lysate was transferred to clean tubes and either homogenized for gradients (see below), mixed with 2X sample buffer or immunoprecipitated. For the immunoprecipitation experiments, lysate was incubated overnight with or without antibody and then rotated with protein A sepharose beads for 1 - 2 h at 4°C. The beads were spun down and washed 3X with lysis buffer and 1X with PBS. Precipitated protein was eluted in reducing 2X sample buffer. Samples were heated at 100°C for 5 min prior to loading on 10% SDS-PAGE gels.

Biotin labeling experiments were conducted to identify the components of the CD20 complex. Cell surface proteins of intact Raji cells (1 X 10^7 cells/sample) were biotinylated using 40 μg E-Z link Sulfo-NHS-LC-Biotin (Pierce) for 10 min at room temperature. Cells were washed four times with 1XPBS and then lysed in 1% digitonin/MBS containing inhibitors as listed above for sample preparation. For biotinylation of total cellular protein, Raji cells were first lysed in 1% digitonin containing the appropriate inhibitors. The lysate was incubated with 75 μg E-Z link Sulfo-NHS-

Biotin for 30 min on ice. The reaction was quenched with 1M TRIS, pH 7.5 for 15 min on ice. Samples were pre-cleared three times for one hour with protein A sepharose beads and non-immune rabbit IgG and then immunoprecipitated as described above.

F. Velocity Gradient Centrifugation

Velocity gradient centrifugation was undertaken to investigate the size of the CD20 complex and the requirement for cytoplasmic domains in its formation. Raji B cells or Molt-4 T cells expressing CD20 constructs (5 X 10^7 cells/sample) were lysed in either 1% Triton X-100 or 1% digitonin/MBS including inhibitors as mentioned above. The lysate was layered onto a 5-40% sucrose gradient containing either 1% Triton X-100 or 1% digitonin and inhibitors as appropriate and then centrifuged at 37000 rpm for 17 hrs at 4°C using a SW 41 rotor (Beckman). 0.5mL or 1mL fractions were collected from the top of the gradient. The first fraction taken from each gradient was designated fraction one with subsequent fractions increasing in number. Samples were mixed with 2X sample buffer, heated as above and analysed on 7.5% or 10% SDS-PAGE gels followed by immunoblot. Protein MW standards, run simultaneously on an adjacent gradient, were treated similarly. A protein of the approximate molecular weight of monomeric CD20, ie OVA (45 kDa) was used as the molecular weight standard for Triton X-100 gradients. The molecular weight standards carbonic anhydrase (29 kDa), bovine serum albumin (66 kDa), alcohol dehydrogenase (150 kDa), beta amylase (200 kDa) (SIGMA gel filtration molecular weight markers) were used for determining the molecular weight of the CD20 complex in the digitonin gradients. Western blot analysis and

coomassie staining was used to determine the fractions containing CD20 and the molecular weight standards, respectively.

G. SDS-PAGE, Coomassie Staining and Immunobloting

Samples were separated by SDS-PAGE under non-reducing or reducing conditions and transferred to Immobilon P (Millipore, Bedford, MA) membranes prior to either Coomassie staining or immunoblotting. Prestained MW markers (Life Technologies or New England Biolabs (Beverly, MA)) were run on each gel. For Coomassie staining, membranes were stained with Coomassie Blue Stain (0.1% Coomassie Blue, 10% glacial acetic acid, 50% methanol) for 2 - 5 min, destained (10% glacial acetic acid, 50% methanol) for 1 min and then for additional 2 - 5 min. Immunoblots were blocked for a minimum of 1 hr 5%BSA/TTBS, incubated with anti-CD20N, anti-CD20C or anti-CD20C2 Abs for 3 h. After washing the membranes, bound Abs were detected with protein A-horseradish peroxidase (Bio-Rad, Richmond, CA). Biotinylated proteins were detected using avidin-horseradish peroxidase (Southern Biotechnology, Birmingham, AL). Proteins were visualized using enhanced chemiluminescence (Pierce) recorded on Kodak X-OMAT film (Eastman Kodak, Rochester, NY).

III. CD20 MEMBRANE ORIENTATION

A. Introduction

For the epitope mapping studies, the residues present in the CD20 extracellular domain had to be confirmed. Human CD20 and its murine equivalent, Ly-44, have been cloned, and their genetic sequences have been characterized (82, 103-105). Based on hydrophobicity data and the lack of a signal sequence, CD20 was predicted to have intracellular N- and C-termini, four transmembrane spans (TM1-4), an extracellular loop between TM3 and TM4 and a possible short loop between TM1 and TM2 (82, 104). Also, since signal sequences are not always necessary for extracellular localization of N-terminal regions (84-89), the predicted membrane orientation of CD20 required confirmation.

A variety of methods for determining the membrane topology of integral membrane proteins have been described in the literature. A method which has been used extensively is the protease digestion of exposed peptide residues on intact cells or in vitro translated protein embedded in microsomal membranes. This involves the use of a membrane-impermeable protease and subsequent analysis of digest fragments by SDS-PAGE and Western blot analysis. For example, the membrane orientation predicted by hydropathy plot analysis of the tetraspan family member CD81 (TAPA-1) was confirmed by in vitro translation of [S^{35}]-labeled protein in the presence of microsomal membranes and subsequent proteolysis. Based on the size of the resulting fragments as

visualized by Western blot, it was concluded that CD81 had intracellular N- and C-terminal regions, four transmembrane domains and two extracellular loops (106).

Another method for determining the membrane topology of integral membrane proteins is the insertion of N-glycosylation sites into the protein sequence. This method is useful since only those sites which will be exposed at the cell surface can be glycosylated. Constructs where N-glycosylation consensus sequences have been introduced are expressed in mammalian cells. Changes in glycosylation indicating extracellular localization would be reflected by shifts in the molecular weight of the protein after SDS-PAGE and Western blot analysis. The predicted membrane topology of the glycine transporter GLYT1 was refuted using this method (107).

Epitope insertion has been utilized in determining the topology of more complicated integral membrane proteins. This method involves the insertion of a small antigenic peptide epitope in predicted intracellular or extracellular loops of the protein. The full-length mutant constructs are expressed in mammalian cells. The position of the inserted epitope is then determined by immunofluorescence of intact or permeabilized cells using epitope-specific antibodies. The topology of mouse P-glycoprotein containing twelve putative transmembrane domains was finally confirmed using this method after a variety of other techniques gave inconsistent results (108).

The membrane topology of the integral membrane protein VIP21 was confirmed by utilizing existing epitopes. Instead of incorporating epitopes into the protein, antibodies were generated against peptide sequences in its N- and C-terminal domains. Affinity purified N- and C-terminal antibodies were then used in determining the

intracellular localization of their epitopes following immunofluorescence of intact and permeabilized cells (109).

Two of these methods were utilized to confirm the membrane orientation of CD20. In this study, Abs generated against peptides in the N- and C-terminal regions of CD20 were used for immunofluorescence of permeabilized cells and for Western blot analysis of protease digest fragments from intact cells.

B. Results

1. Specificity of CD20N and CD20C Abs

To determine the membrane orientation of CD20, Abs against known epitopes were generated in rabbits by immunization with OVA-conjugated CD20 N and C region peptides. The resulting antisera, anti-CD20N and anti-CD20C, were affinity purified and tested for specificity before use in membrane orientation studies. Specificity was confirmed in three ways. First, both antisera detected proteins of 33 to 35 kDa in immunoblots of whole cell lysates derived from Raji B cells (Figure III.1A). CD20 migrates on SDS-PAGE as a single band, a doublet or a triplet depending upon the quantity of protein present and the resolving power of the gel. The differently migrating species are the result of differential serine/threonine phosphorylation (76). Preincubation of the Abs with the immunizing peptides inhibited binding, while incubation with irrelevant peptides did not (Figure III.1A). Second, immunoprecipitation with anti-CD20N and detection by immunoblotting with anti-CD20C demonstrated that both Abs recognized epitopes on the same protein (Figure III.1B). Third, both Abs specifically

recognized CD20 ectopically expressed by transfection in the Molt-4 T cell line (Figure III.1C).

*2. **Confirmation of the Membrane Orientation of CD20***

Localization of the N- and C-terminal regions of CD20 was assessed by indirect immunofluorescence using intact and membrane-permeabilized Raji B cells. CD20N and CD20C Abs did not recognize CD20 on intact cells (Figure III.2). However, after permeabilization there was a specific increase in intracellular staining by both anti-CD20N and anti-CD20C Abs that was prevented by pre-incubation of the Abs with immunizing peptide. Effective permeabilization of the cells was confirmed by the detection of the cytoplasmic Src family tyrosine kinase Lyn only after the permeabilization procedure (data not shown). Since the epitopes recognized by anti-CD20N and anti-CD20C were accessible only after permeabilization, these data confirm the intracellular location of both the N- and C-terminal regions of CD20.

The intracellular location of both termini indicates that CD20 must assume one of three possible topologies relative to the plasma membrane (see Figure III.3). Protease digestion of intact cells was performed to evaluate the number and the locations of extracellular loops. Complete digestion of extracellular regions would be expected to result in either 8- or 15kDa N-terminal fragments depending on whether the polypeptide is exposed at the cell surface on the carboxyl side of TM1. For these studies we used both trypsin, which cuts specifically on the carboxylic acid side of arginine or lysine, and the nonspecific protease proteinase K to treat intact Raji B cells as described in Materials

and Methods. There is no trypsin digest site present in the putative loop between TM1 and TM2, and four sites in the hydrophilic region between TM3 and TM4. Therefore, the presence of an extracellular TM1-TM2 loop (Figure III.3ii) would be expected to generate approximately 15- and 8-kDa N-terminal fragments by trypsin and proteinase K, respectively. Further, there are four trypsin sites in the short hydrophilic stretch between TM2 and TM3. These sites would only be exposed in the two transmembrane/one extracellular loop model (Figure III.3i) and would also generate a significantly larger trypsin fragment compared with proteinase K. The only topology that would generate 15-kDa fragments after digestion with either trypsin or proteinase K is shown in Figure III.3iii.

The size of the smallest N-terminal fragment generated by digestion of intact cells with either trypsin or proteinase K was slightly >15 kDa (Figure III.4), indicating that the protein does not exit to the cell surface between TM1 and TM3, and that there is a single extracellular loop between TM3 and TM4 (Figure III.3iii). Recognition of more than one band in both the trypsin- and proteinase K-digested samples by CD20N Ab is probably due to serine/threonine phosphorylation as seen in the intact protein. Incomplete digestion by trypsin may account for the third and largest N-terminal fragment detected. Fragments obtained after proteinase K digestion were slightly smaller than that obtained after trypsin digestion, as expected due to clipping of a few extra residues between the most N-terminal trypsin cut site and the outer leaflet of the plasma membrane.

The size of the C-terminal fragments (~21 kDa) resulting from digestion by either trypsin or proteinase K significantly exceeded the expected size (14 kDa), but is too large

to be accounted for by incomplete digestion of the extracellular loop. The discrepancy in size may be attributable to post-translational modifications in the C-terminal region, such as phosphorylation and/or acylation, or to SDS-resistant protein-protein interactions occurring after digestion. There are multiple potential phosphorylation sites in the cytoplasmic C-terminal region and CD20 is known to be phosphorylated constitutively (110, 111), and the level of phosphorylation is increased upon activation with phorbol esters (PMA) or Abs directed against surface IgM (111-114). The phosphate groups present constitutively or resulting from post-digest phosphorylation may have affected the migration of the CD20 C-terminal digest fragment.

As well, the membrane proximal C-terminal residues 219-252 required for redistribution includes a cysteine residue at position 220 which may be a site for palmitoylation. Although palmitoylation of this cysteine residue is not required for CD20 redistribution, this cysteine residue may be palmitoylated thereby affecting the migration of the C-terminal digest fragment.

The results of this study have been published (90).

C. Discussion

Since the epitopes recognized by anti-CD20N and anti-CD20C were not destroyed by protease digestion, these results, together with those in Figure III.2, confirm their intracellular location. Data from extracellular protease digestion analyses confirm a four-TM domain topology with a single extracellular loop between TM3 and TM4, in agreement with the hydropathy prediction.

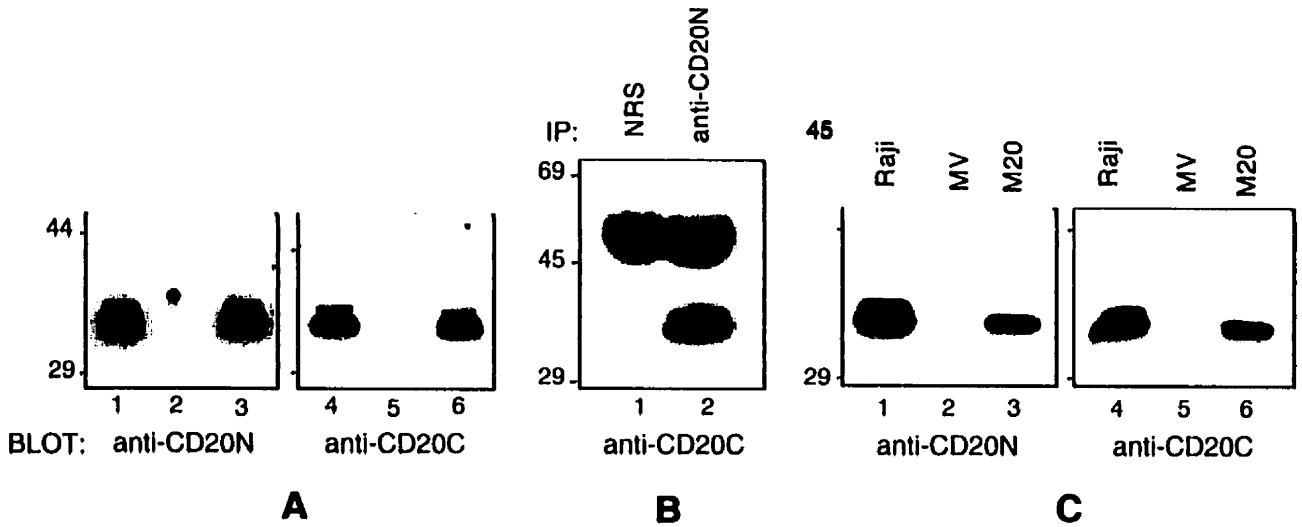

FIGURE III.1. Specificity of anti-CD20N and anti-CD20C Abs for CD20. *A.* Whole cell lysate prepared from Raji B cells was separated on 10% SDS-PAGE and then immunoblotted with anti-CD20N or anti-CD20C Ab, either untreated (lanes 1 and 4) or previously incubated with immunizing peptide (lanes 2 and 5) or irrelevant peptide (lanes 3 and 6). *B.* Whole cell lysate prepared from Raji B cells was immunoprecipitated with either normal rabbit serum (NRS; lane 1) or anti-CD20N Ab (lane 2), separated on 10% SDS-PAGE, and then immunoblotted with anti-CD20CAb. The bands above the 45 kDa marker are rabbit heavy chain. *C.* Whole cell lysates prepared from Raji B cells (lanes 1 and 4) or Molt-4 T cells transfected with either vector alone (MV; lanes 2 and 5) or CD20 cDNA (M20; lanes 3 and 6) were separated on 10% SDS-PAGE and then immunoblotted with anti-CD20N or anti-CD20C Ab.

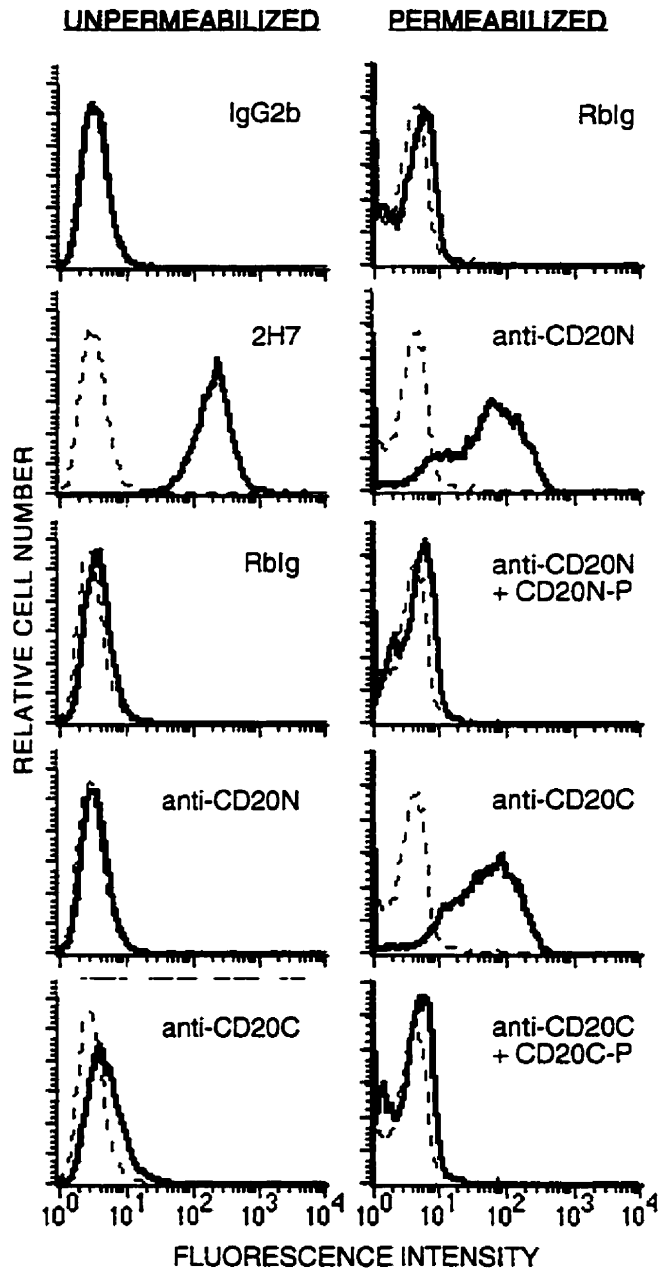

FIGURE III.2. Anti-CD20N and anti-CD20C Abs recognize intracellular epitopes. Indirect immunofluorescence was performed on untreated and saponin-permeabilized Raji B cells. Dashed line profiles show binding of the FITC-labeled secondary Ab alone. Solid line profiles show binding of the primary Abs indicated.

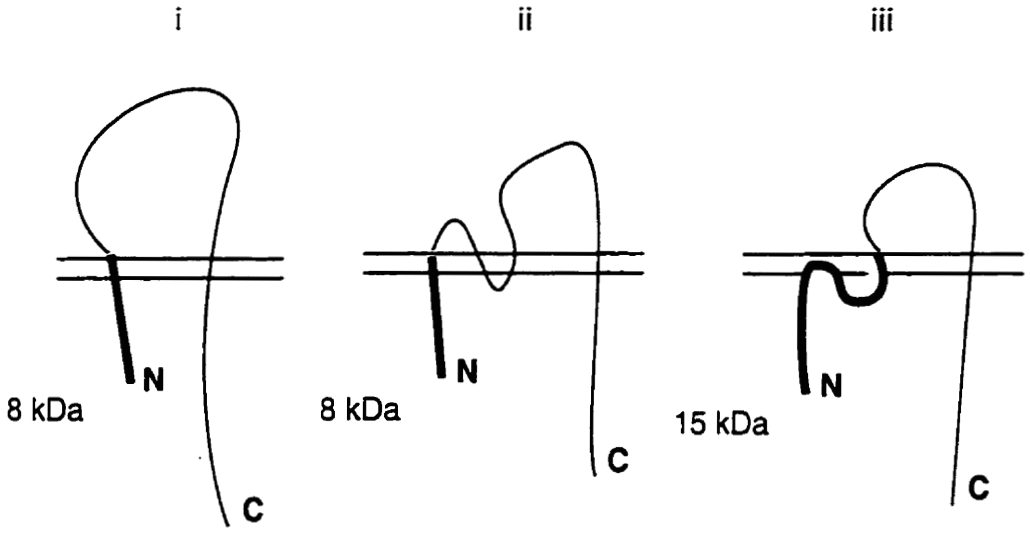

FIGURE III. 3. CD20 topology. Only three topologic orientations (*i-iii*) of CD20 are possible with intracellular N- and C-termini and a long hydrophilic stretch proximal to the most C-terminal transmembrane span. Complete digestion of extracellular regions would yield N-terminal fragments (bold lines) of the sizes indicated. Protease digestion data supports the topology shown in *iii*.

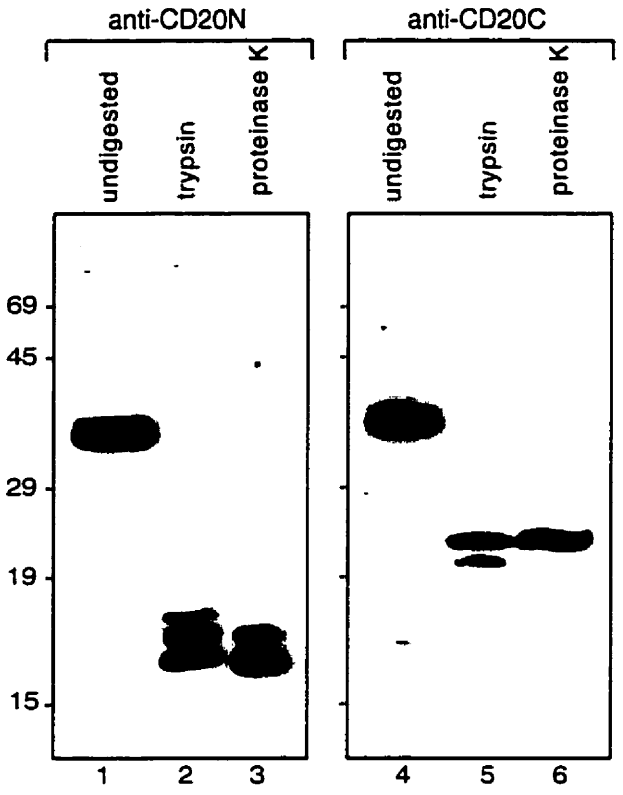

FIGURE III. 4. Trypsin and proteinase K digests of CD20. Raji B cells were either untreated (lanes 1 and 4) or digested with trypsin (lanes 2 and 5) or proteinase K (lanes 3 and 6) before lysis. Samples were separated on 12.5% SDS-PAGE and immunoblotted with anti-CD20N or anti-CD20C Ab as shown.

IV. CD20 COMPLEX

A. Introduction

As described in chapter I, the various effects of the mAbs directed against the extracellular region suggest a more complex fine specificity of mAb binding than previously recognized. Since there are few differences between murine and human CD20, it is possible that some epitopes could be composed of residues on adjacent molecules. If the epitopes span adjacent molecules, then there are two possibilities for the composition of these epitopes. 1) The epitopes could be composed of pre-existing complexes or 2) CD20 molecules aggregate upon mAb binding. The various antibodies could recognize or cause aggregation into different populations of CD20 complexes. To examine the size and complexity of CD20 prior to mAb ligation, velocity gradient centrifugation was utilized.

Velocity gradient centrifugation is a method whereby native protein complex size is determined by its localization to regions of similar density in a linear sucrose gradient after solubilization in detergent. This method has been used to determine the size of several transmembrane protein complexes including stomatin (115) and MAL oligomers (116) and to examine the composition of the epithelial Na+ channel (117). Solubilizing detergent is present in the gradient to prevent its dilution and thereby non-specific aggregation of proteins.

Protein complex preservation is dependent upon the detergent and the nature of the protein-protein interactions in the complex. As a result, detergents differentially preserve the complexity of transmembrane and associated proteins. For example, the

BCR complex, surface IgM (sIgM) or sIgD with Igα and Igβ, is labile in NP-40 (118, 119), but is preserved in digitonin (120). Association of additional components such as lyn are preserved in β octyl glucoside (121).

As well, the detergent-dependence of the tetraspan web has aided in elucidating its organization. The tetraspan web is comprised of tetraspan superfamily members including CD9, CD53, CD63, CD81 and CD82 in multimolecular complexes with β1 integrins and MHCII (122). These associated molecules were identified by co-precipitation with the tetraspans in mild detergents such as Brij 97 or CHAPS (122). The association of the tetraspans CD81 and CD151 with integrins are maintained in digitonin, however, the association between integrins and other tetraspan family members are disrupted (123). This suggests that the other tetraspans interact with integrins via CD81 and CD151.

The CD19 complex, including CD21 and the tetraspan CD81, is involved in the amplification of B cell activation signals (25, 24). In the presence of Brij97, CD19 was shown to be associated with additional tetraspan molecules CD9 and CD82. The association of CD19 with both CD9 and CD82 was disrupted in digitonin, while its association with CD81 was maintained suggesting that its association with those two tetraspans is via CD81 (124).

B. Results

1. CD20 is a monomer in Triton X100

Previous chemical cross-linking studies indicated that CD20 may exist as a monomer, dimer and tetramer (95). In order to examine the CD20 complexes present in Triton X-100, proteins in Raji cell lysate were fractionated by velocity gradient centrifugation. CD20 localized to fractions corresponding to the size of a monomer when compared to molecular weight standards run simultaneously on an adjacent gradient (Figure IV.1).

2. CD20 exists as a ~200kDa oligomeric complex in digitonin

The existence of CD20 as a monomer under non-denaturing conditions in the presence of Triton X-100 was not consistent with the chemical cross-linking results. As mentioned previously, the structural integrity of transmembrane protein complexes is detergent-dependent. Detergents which are less able to solubilize membranes are more capable of maintaining the integrity of transmembrane protein complexes implying that the remaining lipid is responsible for complex stability (125). The mild detergent digitonin is stringent enough to disrupt major oligomeric complexes which are kept intact in other mild detergents (123), but can maintain the integrity of complexes which are labile in harsh detergents (118, 119, 121). As mentioned previously, the BCR complex is one such example where the complex is kept intact in digitonin or β octyl glucoside (121), but not in NP-40 (118, 119). Since this complex could be maintained in digitonin, complexes

sensitive to harsh detergents including Triton X-100 could possibly be maintained in digitonin. As a result, digitonin was then utilized to examine the size of the CD20 complex.

Raji cells lysed in digitonin were fractionated on a sucrose gradient containing digitonin. The results showed that CD20 localized to a fraction corresponding to greater than 150 kDa when compared to the cytoplasmic internal control PLCγ and of ~200 kDa when compared to molecular weight standards run in an adjacent gradient (Figure IV.2). Although sucrose gradients have been successfully used to distinguish several species of complex including monomers, dimers, and tetramers (ie. MAL) (116), only a single CD20 complex was detected. In order to confirm that this was not an artefact of the detergent, the same samples were examined to determine whether gp130, a transmembrane cytokine receptor component that exists as a 130 kDa monomer when unstimulated, migrated as a monomer. Indeed, gp130 fractionated to regions of the gradient corresponding to less than 150 kDa (data not shown).

This result supports the existence of CD20 tetramers as shown by chemical cross-linking, but not of CD20 monomers or dimers. There are possibly two reasons for this result. 1) The conditions used in the chemical cross-linking studies may have been less stringent than those utilized in the velocity gradient experiments to allow for the identification of the CD20 complex constituents. Indeed, preliminary studies have indicated that CD20 is capable of forming dimers under non-reducing conditions *in vitro* (Figure IV.3). It is very possible that the tetramers observed in the velocity gradient

experiments are dimers of such dimers. 2) The concentration and/or nature of detergent used in our studies may not have allowed the various populations to be distinguished. Other studies, however, have shown that the majority of protein associations are disrupted in digitonin (117, 121, 124) suggesting this detergent is more stringent than others and that the size of the CD20 complex is correct.

3. CD20 cytoplasmic regions are not required for complex formation

Previously in our laboratory, it was demonstrated that CD20 redistribution to lipid rafts is dependent upon the cytoplasmic membrane proximal amino acids 219 to 252 in the C-terminal region (90). To determine whether these or other cytoplasmic residues might be involved in CD20 complex formation, several already established cytoplasmic deletion mutants stably expressed in Molt-4 T cells were tested for their ability to form complexes (Figure IV.4). The deletion construct lacking the entire N-terminal cytoplasmic region (NΔ1-49) was detected using the polyclonal anti-CD20C2 antibody. Since a mutant lacking the entire C-terminal region could not be expressed successfully, the effect of the C-terminal region was examined using two constructs, CΔ219-252 and CΔ253-297, that were detected in immunoblots using the polyclonal anti-CD20C2 and anti-CD20N antibody, respectively. If any of these regions is involved in CD20 complex formation, then CD20 mutant complex localization would be affected during velocity gradient centrifugation after solubilization in digitonin.

Velocity gradient centrifugation of the deletion mutants demonstrated no substantial effect on complex size. The slight shifts observed reflected the differences in the molecular weight of the CD20 mutants. Deletion of the membrane distal forty-five amino acid residues in the C-terminal region (CΔ253-297) had no effect on CD20 complex formation as this deletion mutant localized to a fraction corresponding to ~200 kDa (Figure IV.5).

Both NΔ1-49 and CΔ219-252 migrated primarily in a fraction corresponding to ~200kDa, however, a minor population (~9%) of each of these mutants appear to have migrated at a molecular weight corresponding to monomers or dimers suggesting these regions may be involved in complex formation. It is possible that the presence of this minor population may represent non-specific binding of the anti-CD20C2 antibody. This issue could have been addressed by preincubating the antibody with immunizing peptide followed by immunoblot of the same samples to determine the specificity of these bands. Regardless of the possibly minor role of the N-terminal and membrane proximal C-terminal residues, these results suggest that the cytoplasmic domains are not essential for CD20 complex formation.

4. CD20 complex is comprised primarily of CD20 with a ~45kDa minor component

In order to identify the components of the CD20 complex, either cell surface proteins or whole cell proteins of Raji B cells were biotinylated before immunoprecipitation of CD20. To examine the presence of proteins with extracellular

domains in the complex, intact Raji cells were biotinylated, lysed in digitonin and then immunoprecipitated with anti-CD20N antibody. Comparison of the anti-CD20N precipitated sample with sample precipitated with sepharose beads alone or with non-immune rabbit IgG negative controls indicated that no biotinylated transmembrane species co-precipitated with CD20 (Figure IV.6, left panel). Since reblotting with anti-CD20N antibody confirmed that CD20 was precipitated, this suggested that CD20 and possibly other proteins present in the complex are poorly cell-surface biotinylated as a result of either absence of an extracellular domain or have few amino residues available for biotinylation.

Poor cell surface biotinylation of CD20 is consistent with numerous experiments conducted in our lab. Although we had demonstrated CD20 has a single extracellular loop(90), its forty-four amino acid extracellular domain is small and contains only four primary amines available for reaction with the biotin derivative. Of these primary amines, one is presumably even less accessible than the others because of its proximity to the membrane. Not only does CD20 have few primary amines available for biotinylation, its small extracellular domain is even less accessible to the biotin derivative since most other B cell surface proteins have substantially larger extracellular domains. As a result, although CD20 is a transmembrane protein, cell surface biotinylation would not necessarily allow it to be identified as such. Similarly, cell surface proteins associated with CD20 may also be poorly biotinylated or, conversely, there may not be any transmembrane proteins present in the complex. Biotinylation should have been controlled for by immunoprecipitating a transmembrane protein known to have a large

extracellular domain with many biotin-reactive residues such as CD45 or MHCII, however, this procedure has consistently yielded strongly biotinylated CD45 and MHCII product in other experiments in this lab.

In order to examine the proteins involved in the complex, total Raji cell digitonin lysate was biotinylated and then immunoprecipitated. Despite pre-clearing the lysate three times with protein A sepharose beads and non-immune rabbit IgG, many biotinylated proteins were non-specifically precipitated with anti-CD20N antibody as compared with sample precipitated with either protein A sepharose beads or non-immune rabbit IgG alone. Two proteins were precipitated specifically with anti-CD20N antibody (Figure IV.6, right panel). The primary biotinylated protein was ~33 kDa in size. A very faintly biotinylated protein of ~45kDa in size was also present. Western blot analysis confirmed the presence of CD20. These results indicate that the major component of the CD20 complex is likely CD20 suggesting a homooligomer. A minor ~45kDa component also appears to be present in the complex.

C. Discussion

1. CD20 Complex: Real or Detergent Artefact?

CD20 exists in a ~200 kDa complex probably comprised of at least four 33 kDa CD20 monomers with a minor ~45 kDa component. The CD20 complex was labile in Triton X-100, but maintained in digitonin. Although the aggregation of CD20 may be an artefact of the detergent, there are several arguments to support the result.

The ability of a transmembrane protein complex to be kept intact is partially dependent upon the detergent utilized to solubilize the plasma membrane. Detergents that are most effective at solubilizing plasma membranes are also most successful at disrupting complexes. This implies that the lipid remaining after detergent solubilization plays an important role in complex stabilization (125).

The harsh non-ionic detergent Triton X-100 was more effective at solubilizing the plasma membrane in this case and, thereby, disrupted the CD20 complex. Digitonin is a mild non-ionic detergent which permeabilizes plasma membranes by complexing membrane cholesterol and other unconjugated β-hydroxysterols when used at concentrations of 0.01% to 0.1% (126). In the velocity gradient experiments conducted here as well as in the literature, a higher concentration of 1% digitonin was utilized to isolate and maintain transmembrane protein complexes. Examples include the dopamine D1 receptor complex (127) and the BCR complex (120). Although other mild detergents such as Brij97 and CHAPS also have been utilized to maintain transmembrane protein complexes (124, 122), digitonin is more stringent and has been used to dissect the specific protein interactions which exist within these complexes. As stated in the introduction for this chapter, the association of the CD19 complex via CD81 with the tetraspans CD9 and CD82 was identified using digitonin (124).

2. Involvement of Cytoplasmic Regions

Complex formation does not appear to be dependent on the cytoplasmic N- and C-terminal regions, since deletion mutants still form complexes. N-terminal and membrane proximal C-terminal residues may be involved in complex formation to a minor extent. As well, the involvement of residues in context of the entire C-terminal region cannot be dismissed. Since the CD20 C-terminal region could not be deleted in its entirety without losing expression (71), the involvement of C-terminal residues could not be eliminated. Although deletion of either of the two adjacent stretches of C-terminal residues had no appreciable effect on CD20 complex formation, deletion affects may have been compensated for by the remaining residues. Since the anti-CD20N and anti-CD20C antibodies, which were generated against peptides in the N- and C-terminal regions, respectively, were successfully utilized in intracellular staining unstimulated B cells, it is unlikely these regions are involved in complex formation. Complex formation is more likely to be dependent upon protein-protein interactions involving the transmembrane or extracellular domains.

3. The ~45 kDa Protein

Analysis of the CD20 complex indicated that the primary component is CD20 with a minor ~45 kDa component. A protein of similar molecular weight has been shown to co-precipitate with CD20 previously (128). Several 50 to 65 kDa cytoplasmic proteins as well as a 31 kDa and a 200 kDa cell surface protein were also shown to be associated with CD20 (128). The 50 to 65 kDa proteins were subsequently identified as

being src family kinases (71), while the 31 kDa and 200 kDa proteins have not yet been identified. The co-precipitation of only the ~45 kDa protein with CD20 with the absence of the proteins listed above may have resulted from the stabilization of hydrophobic interactions by digitonin. Certain CD20 associations may be enhanced in certain detergents, but eliminated by others. For example, CD20 can associate with MHCII in CHAPS, but this association is disrupted in NP40 buffer (56). As well, the 31 kDa and 200 kDa proteins may be indirectly associated with CD20. These other proteins may also be in lower abundance in the membrane, thereby, associating with a smaller population of CD20.

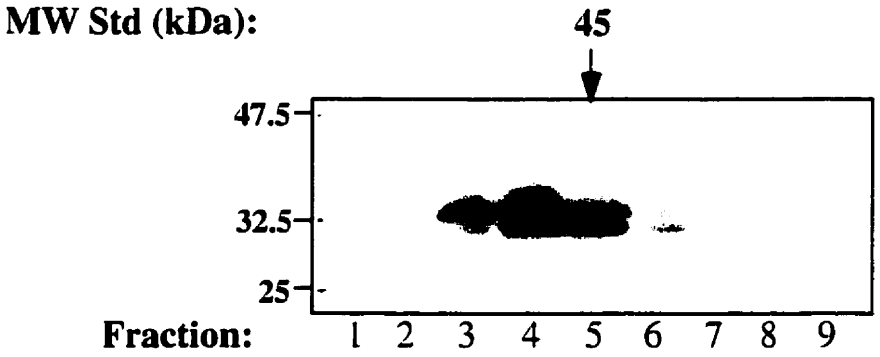

FIGURE IV.1. CD20 migrates as a monomer on a 1% Triton sucrose gradient. Fractions of B cells lysed in 1% Triton X-100 were analysed by SDS-PAGE and anti-CD20N immunoblot after separation by velocity gradient centrifugation. CD20 localized primarily to fraction 4 corresponding to a molecular weight < 45 kDa upon comparison with molecular weight standards separated on an adjacent gradient. (n=3)

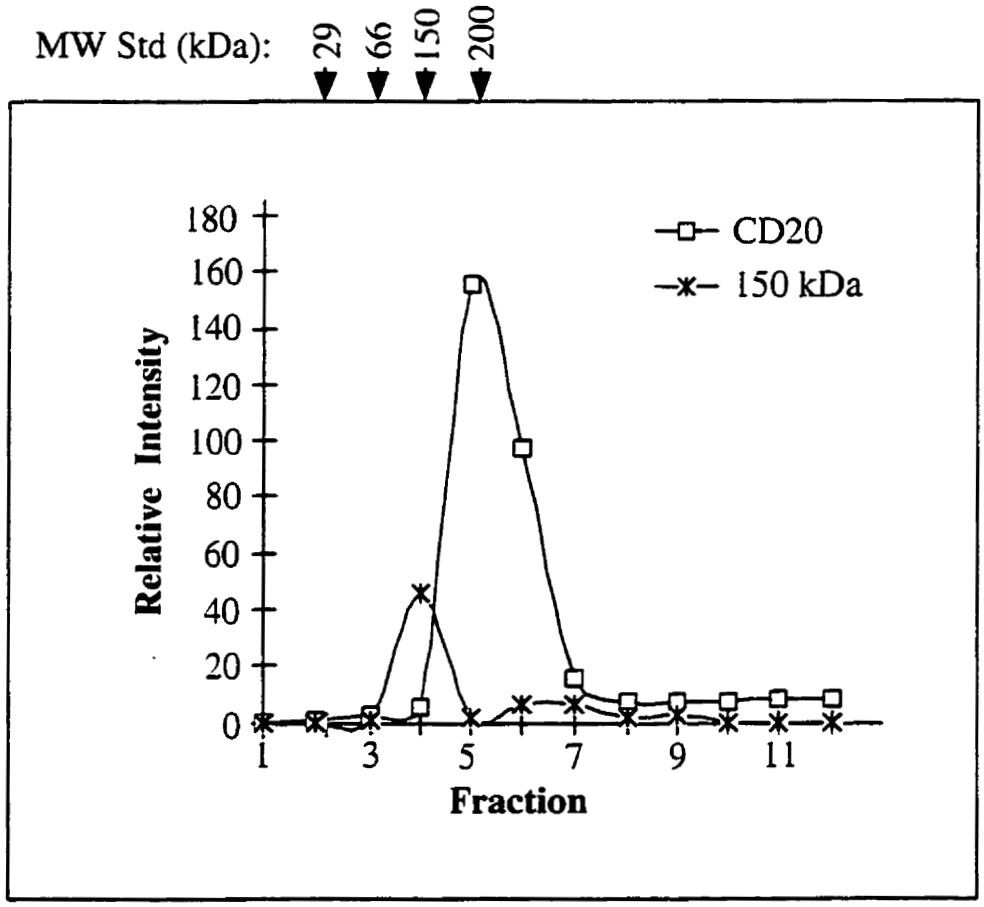

FIGURE IV.2. CD20 complex is greater than 150 kDa. Fractions of Raji B cell lysate were analysed by SDS-PAGE and immunoblot after separation by velocity gradient centrifugation on 5-40% sucrose/ 1% digitonin. The MW of the CD20 complex was shown to be greater than 150 kDa by comparison to an internal protein standard and MW standards run simultaneously on an adjacent gradient. (n=4)

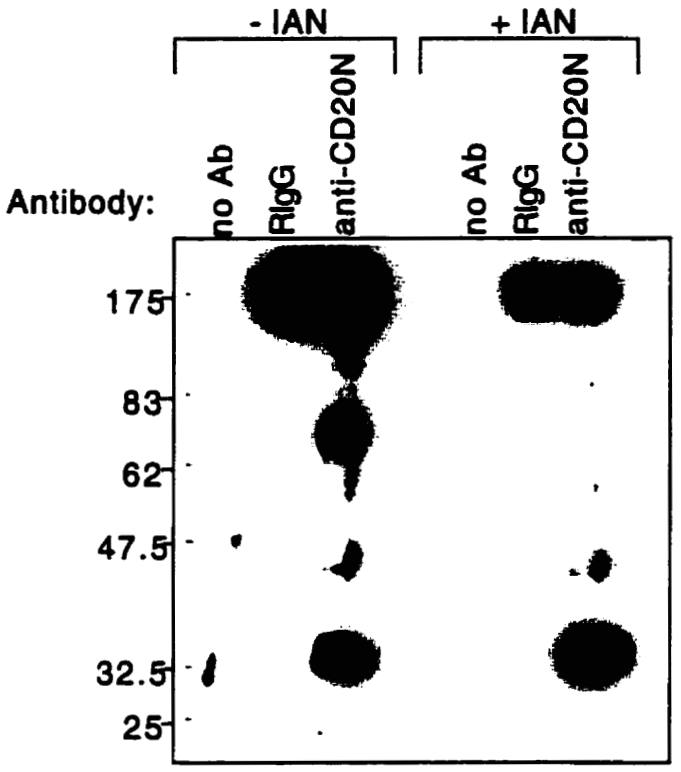

FIGURE IV.3. CD20 forms dimers under non-reducing conditions *in vitro*. CD20 was preciptated from Raji cells lysed in 0.5% Triton X-100 (1×10^7 cell equivalents/sample) with either no Ab, non-immune rabbit IgG (RIgG) or anti-CD20N Ab (0.5 µg Ab/sample). Precipitation was carried out with or without 100 mM iodoacetamide (IAN). Iodoacetamide prevents the formation of disulfide bonds by reacting with free sulfhydral groups. Samples were separated on 7.5% SDS-PAGE and analysed by anti-CD20N western blot.

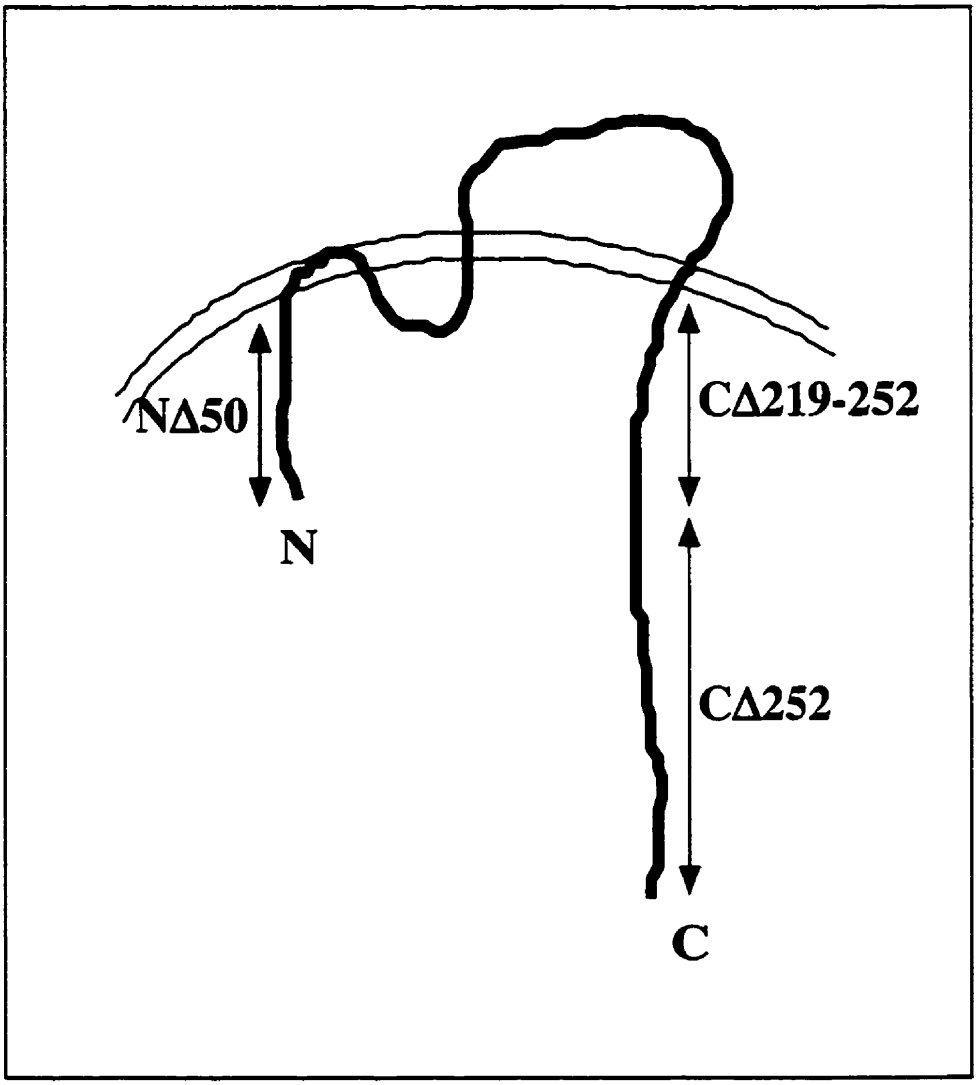

FIGURE IV.4. CD20 cytoplasmic deletion mutants. Positions of cytoplasmic deletions in the N- and C-terminal domains of CD20 are indicated. Deletion mutants stably transfected into Molt-4 T cells were used for analysis of the requirement of cytoplasmic regions in CD20 complex formation.

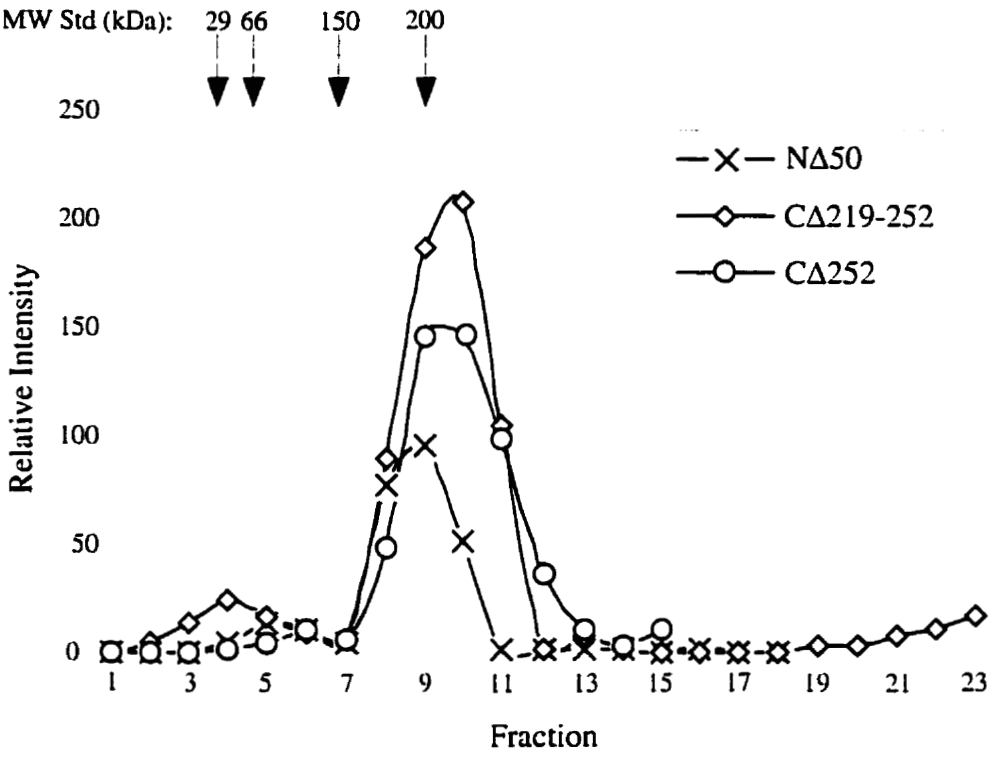

FIGURE IV.5. CD20 cytoplasmic deletion mutants form ~200 kDa complexes. Fractions of Molt-4 CD20 cytoplasmic mutant T cell lysates were analysed by SDS-PAGE and immunoblot after separation by velocity gradient centrifugation on 5-40% sucrose/1% digitonin. Complex molecular weight was determined by comparison to standards run simultaneously on an adjacent gradient. (n=1)

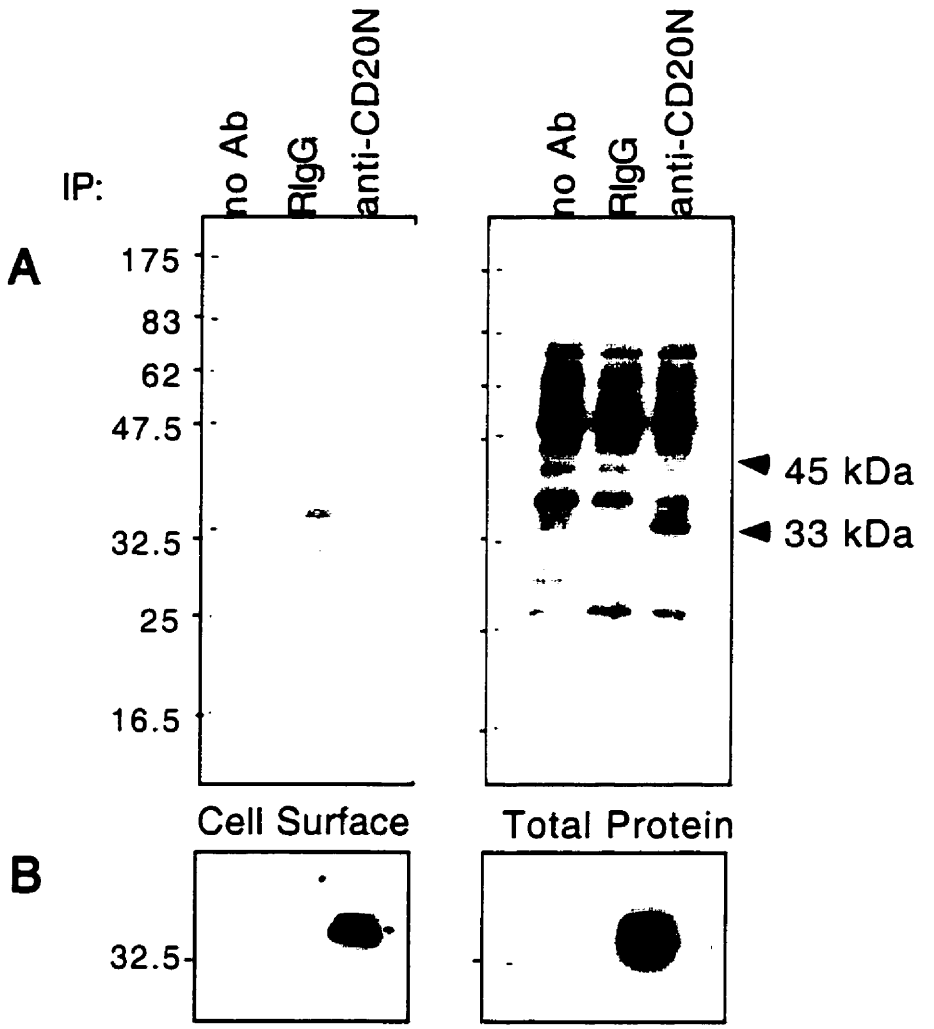

FIGURE IV.6. CD20 complex is heteroligomeric having a 33 kDa major component and a ~45 kDa minor component. *A*. Cell surface proteins (left panels; n=2) or total proteins (right panels; n=3) of Raji B cell lysate were biotinylated and then immunoprecipitated with either no antibody (Ab), non-immune rabbit IgG (RIgG) or anti-CD20N antibody. Samples were analysed by SDS-PAGE and immunoblot. Total biotinylated protein samples were pre-cleared with sepharose beads and RIgG three times. *B*. Anti-CD20N antibody blot of the same samples to confirm presence of CD20.

NOTE: ~45 kDa protein is difficult to see in scanned image, but is clearly present on original film.

V. EPITOPE MAPPING

A. Introduction

As was shown in the last chapter, CD20 exists in an oligomeric complex comprised primarily of CD20. This lends more support to the premise that the anti-CD20 mAbs do indeed recognize unique epitopes of adjacent molecules. Several epitope mapping strategies were then undertaken to identify the specific amino acids recognized by the anti-CD20 mAbs 1F5, 2H7 and B1.

Epitope mapping is the process of identifying antibody binding sites. Epitopes can be either continuous or discontinuous. Continuous epitopes, composed of a linear sequence of amino acids, are usually resistant to protein denaturation. Discontinuous epitopes, comprised of amino acids separated in the protein sequence, are a result of secondary and/or tertiary structure and are destroyed upon protein denaturation. Some epitopes are not present in the native protein, but are exposed after denaturation. Mapping the epitopes of mAbs can be used for structural and functional characterization of proteins.

A variety of strategies have been used to identify the epitopes of proteins. Initially, it is important to first determine the type of epitope recognized by the panel of mAbs that recognize the desired protein. This can be achieved by Western blotting the protein with a panel of mAbs to determine which ones recognize denaturation resistant epitopes (129).

Next, in order to identify possible antigenic sites, computer analysis can be undertaken to predict the protein secondary structure and regions of greatest antigenicity. Antibody binding of the panel of mAbs to related proteins can also be undertaken to determine if the epitopes recognized are conserved or unique (129).

A general epitope map can be derived using cross-blocking or proteolysis of the anitgen-antibody complex. Cross-blocking can be utilized to determine if the mAbs bind identical or overlapping regions. Experimentally, this can be achieved by pre-incubating the protein with a member of the mAb panel and monitoring its ability to block the binding of other mAbs (129, 130). An epitope map can also be derived using a protease with limited, known cut sites to digest antigen-antibody complexes. Because antibody protects its antigen from proteolysis, fragment sizes resulting from digestion of protein pre-treated with antibody can aid in elucidating an epitope map (131).

In cases where some or all of the members of the antibody panel recognize a continuous epitope, peptide inhibition can be used to determine the epitopes. Peptides derived from the surface of proteins or, in the case of integral membrane proteins, from extracellular regions can be generated synthetically or by digestion. Pre-incubation of antibodies with the peptides and the degree to which the peptides block antibody binding to the desired protein can be utilized to deduce the epitopes recognized by each antibody (129). For example, to understand the structure of the adult rat skeletal sodium channel, mAbs were generated and then their epitopes identified using mAb binding to channel proteolytic fragments (132-134) and by quantitative inhibition of mAb binding to synthetic oligopeptides (135).

Homolog scanning and x-ray crystallography can be used to derive a more specific epitope map. Homolog scanning is the systematic or random substitution of amino acid sequences in one homolog with amino acid sequences from another homolog. The gain or loss of binding by antibodies which recognize one homolog but not the other can be used as a powerful tool in mapping epitopes, especially in mapping discontinuous epitopes (136). This technique was initially used to identify the sites for binding of human growth hormone to its receptor and to mAb. It was achieved by systematic substitution of stretches derived from homologous hormones known not to bind the receptor or mAbs (137). Homolog scanning mutagenesis has also been utilized in identifying the residues of the TM4 superfamily pan-leukocyte glycoprotein CD53. Anti-CD53 mAbs recognize rat but not murine epitopes so rat/murine chimeras of the major hydrophilic region of CD53 expressed as a GST fusion protein were used in mapping epitopes and confirming the extracellular localization of the region used in the analysis (138).

X-ray crystallography is essentially the only method for identifying all the amino acids that come in contact with an antibody. This technique has been most successfully used to analyse antigen-antibody complexes of highly conformational epitopes on the surface of soluble proteins. Drawbacks include expense, expertise, time and, importantly, the availability of highly purified, crystallizable protein (139).

Two epitope mapping strategies, homolog comparison and cross-blocking, have already been utilized for epitope mapping of CD20. In order to determine if the epitopes are conserved in homologs, binding of anti-human CD20 mAbs to murine CD20 was monitored. Despite the high degree of homology between the murine and human

sequences, four anti-human CD20 mAbs, 1F5, 2H7, B1 and G28-2, could not recognize the extracellular region of murine CD20 as determined by indirect immunofluorescence (70). Crossblocking experiments were undertaken to measure binding of fluorescently-labelled B1 mAb to CD20 pre-treated with a panel of anti-CD20 mAbs. Nearly all mAbs, including 2H7, blocked the binding of B1 completely suggesting they recognize the same epitope. 1F5 and AP-291 partially blocked B1 binding suggesting these mAbs may bind to a site close to, but distinct from the epitope of B1 (70). These kinds of studies are inconclusive, however, since the bound mAb may sterically hinder the binding of the second mAb to its epitope.

As mentioned previously, human CD20 and its murine homolog have been cloned. Of the forty-four amino acids in the extracellular domain, sixteen are non-homologous between the two species (see Figure V.1). Only eight of the sixteen amino acids are non-conservative substitutions, yet anti-human CD20 mAbs do not recognize murine epitopes (105). As well, absence of the use of these mAbs for western blotting in the literature suggests the recognition of discontinuous epitopes.

This information was utilized in combination with epitope mapping strategies used for other integral membrane proteins to map the epitopes of CD20 by 1) identifying the type of epitope recognized using Western blotting and peptide inhibition and 2) determining the amino acids that comprise the epitope by homolog scanning mutagenesis.

B. Results

1. mAbs Recognize Discontinuous Epitopes

The three anti-CD20 mAbs 1F5, 2H7 and B1 had not been used for immunoblotting in the literature suggesting these mAbs may not recognize linear epitopes. To confirm these mAbs recognize epitopes which are not resistant to denaturation, western blotting and peptide inhibition studies were undertaken.

A synthetic peptide of the least homologous stretch of amino acids in the human CD20 extracellular domain (boxed sequence in FigureV.1) was pre-incubated with anti-CD20 mAbs or with antibody isotype controls and their ability to inhibit binding to CD20 expressed on Raji B cells monitored using immunofluorescence. Results demonstrated that 1F5, 2H7 and B1 binding to CD20 was not inhibited after pre-incubation with a vast excess of peptide as compared with mAb incubated without peptide (Figure V.2). This suggests that the peptide sequence chosen for the inhibition studies was not present in the epitopes recognized by any of the antibodies or, more likely, that the antibodies recognize a discontinuous epitope.

In order to confirm that these mAbs recognize epitopes not resistant to denaturation, Western blot analysis was undertaken. CD20 was immunoprecipitated from Raji B cell lysate with anti-CD20N antibody. Samples were separated using denaturing and reducing conditions on SDS-PAGE and then blotted with the anti-CD20 antibodies 1F5, 2H7 and B1 as well as anti-CD20N for a positive control (Figure V.3). Visualization of CD20 by any of the anti-CD20 antibodies would indicate the recognition

of a continuous epitope. Indeed, although CD20 was successfully immunoprecipitated using anti-CD20N as shown by blotting with anti-CD20N, no specific CD20 signal was detected using 1F5, 2H7 or B1. This result confirms the inability of these mAbs to recognize denatured epitopes.

2. Homolog Scanning Mutagenesis: Negative Binding Strategy

2.1 Introduction

Evidence from the peptide inhibition and western blot studies indicated that the epitopes recognized by the panel of anti-CD20 mAbs are likely discontinuous. As a result, homolog scanning was undertaken for epitope mapping CD20. Initially, a negative binding strategy was undertaken in which human CD20 was mutated toward the murine sequence and loss of binding of anti-human CD20 was monitored by immunofluorescence.

2.2 Mutations and Rationale

The human CD20 extracellular domain was converted stepwise toward the murine sequence. Seven mutants were constructed each containing from one to four changes in adjacent non-homologous amino acids as shown in FigureV.4. It was more convenient to construct seven mutants with conveniently grouped changes in adjacent non-homologous amino acids than sixteen mutants, one for each non-homologous amino acid. It was thought that the mutant groupings could provide a hint toward the residues which comprised the epitopes. Based on the results, constructs containing point mutations or a combination of mutants could be constructed.

2.3 Optimization of Transfection Conditions

To directly compare binding of the various mAbs to the CD20 extracellular domain mutants, conditions to achieve maximal and consistent expression of mutants had to be determined. First, transient transfection was chosen over stable transfection because it provides rapid expression of construct within a few days.

Once the use of transient transfection had been decided, the cell line to be utilized for this series of experiments was chosen. The adherent cell line HEK 293 was selected for transient expression of the constructs. The HEK 293 (human embryonic kidney) cell line was developed in 1977 by sheared Adenovirus 5 DNA transformation. This cell line is well characterized and commonly utilized for this purpose in the literature. The cells are easily transfectable using the calcium phosphate method, and preliminary results demonstrated high transfection efficiency (FigureV.5). Also, although these cells are adherent, they could be lifted from substratum gently with washing thereby avoiding the use of EDTA or proteases.

Constructs were transiently transfected into HEK 293 cells using the calcium phosphate method outlined in the Materials and Methods. Transfection conditions were optimized by monitoring expression of various amounts of wild type CD20 over time using FACs analysis. To determine optimal expression over time, 5 μg CD20 cDNA was transfected into ~50% confluent HEK 293 cells and expression monitored one, two, or three days post-transfection. Transfection efficiency was maximal two days post-transfection of cells at ~50% confluence (Figure V.6). Once the time of optimal

expression was determined, the optimal amount of DNA for transfection was determined. Varying amounts (2 to 35 μg) of wild type CD20 cDNA was used for transfection and expression monitored after two days. Expression of CD20 was maximal with 15 μg transfected DNA and did not increase further with higher amounts of DNA (Figure V.7). Since expression varied with minor changes up to 15 μg DNA transfected (inset, Figure V.7), an excess of DNA (~20 μg) was used to minimize variability. Based on these results, for the epitope mapping studies 20 μg DNA was transfected into HEK 293 cells and mAb binding was monitored usually at two days, but on occasion at three days, post-transfection.

Although there was maximal expression under these conditions, there was reduced viability of cells as a result of transfection. In order to eliminate the non-viable cells, samples were treated with propidium iodide. Cells undergoing cell-death would be leaky and internalize the propidium iodide which would intercalate with its DNA and fluoresce at a UV spectrum wavelength of 493 nm. These cells could then be gated out, thus eliminating the population of cells to which mAbs were binding non-specifically, leaving only viable cells to which mAb bound to specifically.

2.4 Results

Cells were lifted from plates two to three days post-transfection and split equally for FACs analysis using the panel of anti-CD20 mAbs and appropriate isotype controls followed by FITC-labelled secondary antibody. An example of the raw data is shown in Figure V.8. Since total median fluorescence values appeared to provide the most accurate

reflection of FACs profiles, these values were used in subsequent experiments for comparing the extent of mAb binding. An example of one complete experiment is shown in Figure V.9. The data indicated that mAb binding to most mutants was diminished, while binding to Mutant 6 was abolished (Figure V.9). These results could have either been an accurate reflection of removal of the epitope recognized by the mAbs or reduced binding because of low construct expression. Although great lengths were taken to ensure that expression was maximal and as a result comparable, there was a possibility that expression of the various constructs was not equivalent.

2.5 Normalization to Expression

In subsequent experiments, antibody binding was normalized for expression. Two to three days after transfection, half the cells from each plate were lysed for western blot analysis, while the rest were split equally for FACs analysis. Equal amounts of protein from transfected cell lysate as determined by modified Lowry method was analysed by SDS-PAGE and anti-CD20N immunoblot. CD20 construct expression was measured by densitometry.

Binding of the various anti-CD20 mAbs to the same transfectants was monitored by FACs analysis. Median fluorescence was normalized for CD20 construct expression as follows. Initially, to obtain net median fluorescence values, median fluorescence of isotype control was subtracted from the median fluorescence of the various anti-CD20 mAbs to each construct. This essentially subtracted background binding. The net densitometry value for each construct was then taken as a ratio of the net densitometry value for wild type. The adjusted median fluorescence was obtained after dividing the net

median fluorescence by the net densitometry value for each construct. Median fluorescence values were normalized by dividing the adjusted median fluorescence for each construct by the adjusted median fluorescence of wild type and multiplying this value by one hundred. This then allowed mAb binding to each construct to be compared directly.

2.6 Normalized Results

In three subsequent experiments where mAb binding was normalized for construct expression, the results were variable except for the reproducible elimination of binding by Mutant 6. The results of one experiment are shown in Figures V.10 and V.11. Western blot analysis showed that all constructs were expressed but at various levels (Figure V.10). The normalized FACs data for this experiment are shown in Figure V.11. Lack of binding to Mutant 6 suggested that the residues altered in this mutant comprised part if not all of the epitopes of the three mAbs tested or that these residues were necessary for providing the secondary structure of the epitopes. Although the results for the other mutants were variable among three experiments, all of the other mutants always bound mAbs, but at reduced levels indicating that a combination of residues was responsible for comprising the different epitopes.

3. Homolog Scanning Mutagenesis: Positive Binding Strategy

3.1 Introduction

Since the results of the negative binding strategy were difficult to interpret, a positive binding strategy was devised to more precisely identify the epitopes recognized by these mAbs. Although this could have most easily been undertaken by starting with

the full-length murine cDNA and converting the extracellular domain toward human, no antibodies against murine CD20 are available to determine expression. A known epitope such as FLAG or myc could have been tagged onto the murine sequence, but I chose to retain the human cytoplasmic domains.

Despite the high degree of homology between cytoplasmic human and murine CD20, anti-CD20N and anti-CD20C antibodies did not recognize CD20 in lysates of murine A20 B cells (data not shown) which had been shown to express CD20 mRNA (105). Because the transmembrane and cytoplasmic CD20 sequences of murine and human are highly conserved, I reasoned that the forty-four amino acid human CD20 extracellular domain could be replaced by the murine sequence without grossly affecting the conformation of the protein. First, the entire human extracellular domain was converted to murine. Surface expression of the chimera was confirmed by protease digestion of the extracellular domain of intact cells (Figure V.12). The murine sequence was then systematically humanized as shown in (Figure V.13). These chimerase had the extracellular murine component necessary for the epitope mapping studies with the cytoplasmic (and transmembrane) human component allowing for detection by Western blot analysis.

3.2 Mutations and Rationale

The mutations were constructed with the intent of maximizing the potential of regaining binding of the various mAbs. Secondary structure analysis of both human and murine CD20 performed using the Npredict program indicated that the N-terminal proximal residues in the extracellular domain form an alpha helix (residues 142-156),

followed by a short stretch of residues which form a β turn and then a final stretch of residues which form another β turn resulting in a structure as shown in Figure V.13. This final β turn includes the ANP sequence which when converted to murine SNS in the negative binding strategy eliminated binding of all three mAbs tested.

These structural components were used as a basis for designing the mutants for the positive binding strategy. Each structural component of the extracellular domain was converted separately toward human to aid in identifying the epitope forming regions. Mutant A corresponded to a predicted extracellular alpha helix. The residues in this contain the majority of unconserved residues in the extracellular domain suggesting an importance in mAb binding. Mutant B contains a stretch of conservative substitutions (VDIYD/INIYN) within the predicted central β turn. It is unlikely these residues directly comprise any epitope since they are conservative substitutions. However, the secondary structure analysis suggests these residues may be involved in secondary structure formation. A mutant containing SNS/ANP, Mutant C, was included because the mutation of ANP in the negative binding strategy had eliminated binding of all three mAbs tested. Since proline residues introduce a kink, it was possible that the effect of the ANP mutation was directly a result of the proline residue within the stretch of amino acids. To test the likelihood of the proline residue independently conferring the secondary structure of the epitopes recognized by the various mAbs, a mutant containing a point mutation of S/P alone, Mutant D (S/P), was included in the study.

3.3 Results

As in the negative binding strategy, these constructs were then transiently transfected into HEK 293 cells by the calcium phosphate method. Surface expression was confirmed using proteinase K proteolysis of the CD20 extracellular domain and fragments detected using the anti-CD20C2 antibody. The detection of appropriate size C-terminal fragments indicated that the extracellular region of each construct was exposed at the cell surface (Figure V.14).

Antibody binding was monitored by indirect immunofluorescence of cells using FITC-conjugated goat anti-mouse antibody. As was expected, 1F5, 2H7 and B1 did not bind to human CD20 containing the murine extracellular domain. Surprisingly, Mutant A, which contained the greatest number of non-homologous residues, did not recover binding by any mAb (Figure V.15). As was expected, the same was the case with Mutant B (VDIYD/INIYN). Although the mutation of ANP/SNS had eliminated binding of the three mAbs tested, mutation of SNS/ANP in Mutant C completely recovered binding of only B1 mAb and slightly recovered binding of 1F5. A point mutation of S/P in this stretch of residues recovered B1 and 1F5 binding slightly. This suggested that the proline residue comprised part, but not all of the epitopes recognized by these two antibodies and that the combination of ANP entirely constituted the B1 epitope. 2H7 binding to Mutant C and Mutant D was similar to that of isotype controls.

C. Discussion

Peptide inhibition and western blot analysis studies confirmed the recognition of discontinuous epitopes by the anti-CD20 mAbs 1F5, 2H7 and B1. A method for identifying the amino acids involved in these discontinuous epitopes, homolog scanning mutagenesis, was then undertaken.

Most of the results obtained for mutants using a negative binding strategy were difficult to interpret because of varied construct expression. Antibody binding to most mutants was affected, while mAb binding was eliminated by ANP/SNS. Not surprisingly, the ANP sequence is within a stretch of amino acids (residues 166-182) predicted to have high antigenicity likely because the proline residue introduces very distinct secondary structure. This proline may comprise part of the epitope or may confer the secondary structure required for the epitope of each mAb.

Although ANP/SNS abolished binding of the three anti-CD20 mAbs in the negative binding strategy, the reverse mutation (SNS/ANP) in a positive binding strategy recovered binding of only one mAb. Mutation of SNS/ANP in the murine CD20 extracellular domain completely recovered binding of only B1. The mutation of S/P alone recovered B1 binding to a lower degree. These results indicate that the B1 epitope is comprised of ANP. Although the western blotting results appear to contradict this finding, the proline in the linear epitope likely provides secondary structure which can be denatured. As well, the identification of these residues as the B1 epitope supports the observation that B1 mAb most easily precipitates CD20 from lysate (data not shown). The epitope is still intact in non-denaturing detergent, since it is comprised of a

continuous stretch of residues having secondary structure. The ability of B1 to precipitate CD20 from Triton X-100 lysate (128) and the nature of its epitope implies that B1 can recognize single CD20 molecules within the complex.

Mutation of SNS/ANP slightly recovered 1F5 binding. This suggests 1F5 recognizes an epitope comprised of ANP and additional unidentified residues.

Since 2H7 binding was not recovered by any of the mutants, the 2H7 epitope is likely comprised entirely of residues dependent upon but not including ANP.

These studies suggest the recognition of unique epitopes by 2H7 and B1, while the epitope of 1F5 and B1 overlap. This finding disproves the cross-blocking experiments which concluded that 2H7 and B1 recognized the same epitope, while 1F5 binds to a distinct overlapping epitope (140).

The lack of binding to Mutant A, although surprising, was consistent with the peptide inhibition studies. The peptide used in these studies is included in the stretch of residues mutated in this construct. The absence of binding to both the peptide and Mutant A do not eliminate the involvement of these residues in mAb binding, but rather suggest the importance of secondary structure imposed by other residues in the extracellular domain.

A different combination of mutations will have to be utilized in a positive binding strategy to completely identify the epitopes recognized by 1F5 and 2H7. Since ANP is important in the binding of all three mAbs, Mutant C (SNS/ANP) would have to be combined with either Mutant A or Mutant B within the same construct. The ANP stretch may be sufficient in providing the secondary structure required for recognition of

additional residues comprising the epitopes of 1F5 and 2H7. Those mutations resulting in higher anti-CD20 mAb binding would have to be examined more closely by mutating single amino acids systematically to determine the specific amino acids important in epitope recognition.

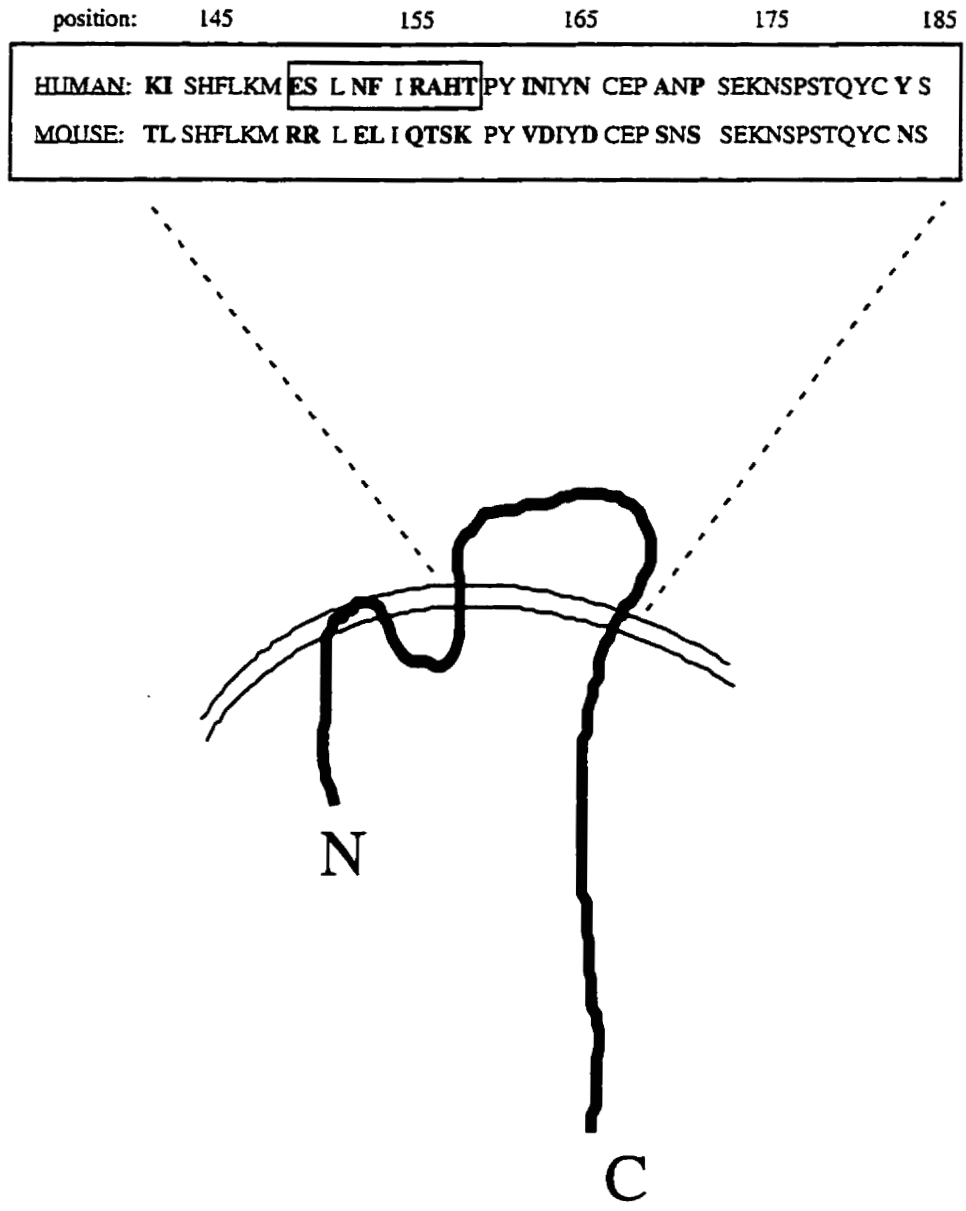

FIGURE V.1. Amino acid sequence of human and murine CD20 extracellular domain. Non-homologous residues are highlighted. Sequence corrsponding to the synthetically generated peptide used in the peptide inhibition studies is boxed.

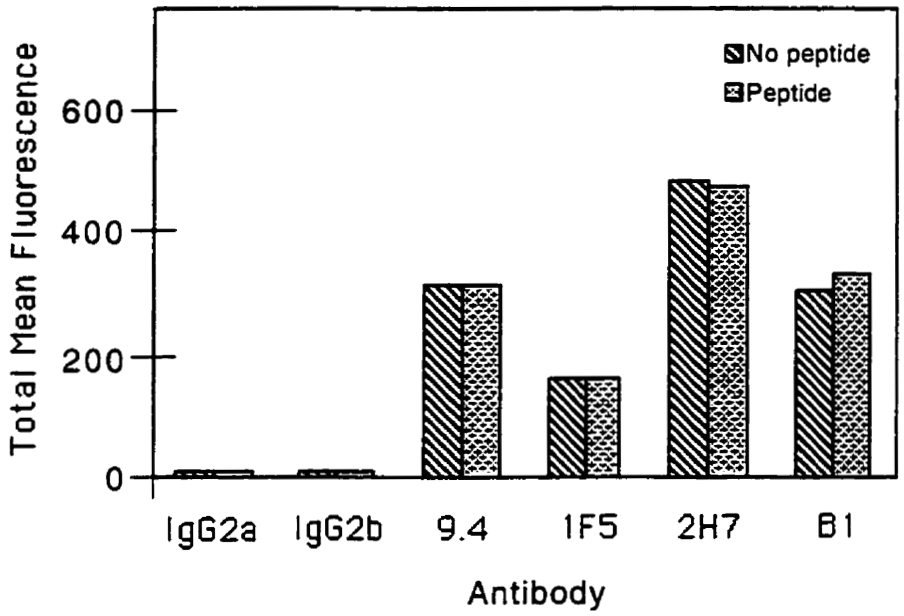

FIGURE V.2. Binding of anti-CD20 mAbs to CD20 was not inhibited by a peptide comprised of the least homologous stretch of the CD20 extracellular domain. Binding of anti-CD20 mAbs, anti-CD45 mAb or isotype controls to Raji B cells was monitored by immunofluorescence. 1 μg of 1F5, 2H7 and B1 anti-CD20 mAb, 9.4 anti-CD45 mAb or isotype control mAbs was pre-incubated with or without 10 μg peptide for 30 min at 37°C (molar ratio 1:135). The peptide used corresponds to a stretch of amino acids least homologous when comparing human and murine sequence (residues 150 -159; ESLNFIRAHT(NH_2)). (n=2)

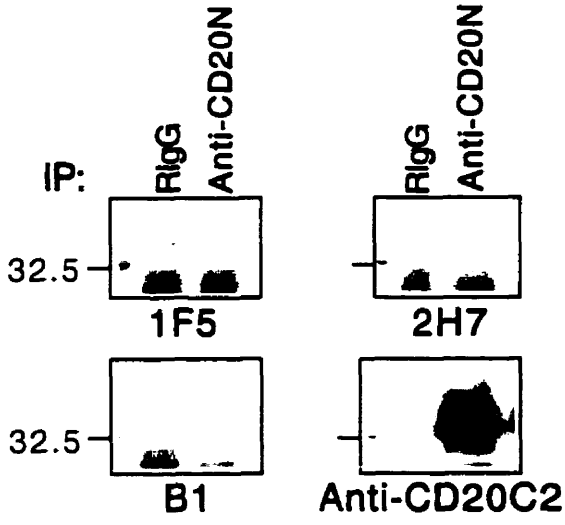

FIGURE V.3. Anti-human CD20 mAbs do not recognize linear epitopes. Raji cell lysate (1 X 10^7 cell equivalents/sample) immunoprecipitated with either non-immune rabbit IgG or anti-CD20N antibody (0.5 µg/sample) was separated by SDS-PAGE and then blotted with either 1F5 (10 µg/mL), 2H7 (10 µg/mL), B1 (10 µg/mL) or anti-CD20C2 (1:10000) antibody. Rabbit anti-mounse-HRP (1:10000) was used as the secondary for the 1F5, 2H7 and B1 blots, while Protein A-HRP (1:5000) was used as the secondary for the anti-CD20C2 blot. Bands at the bottom of the figures are light chain from the precipitating Abs.

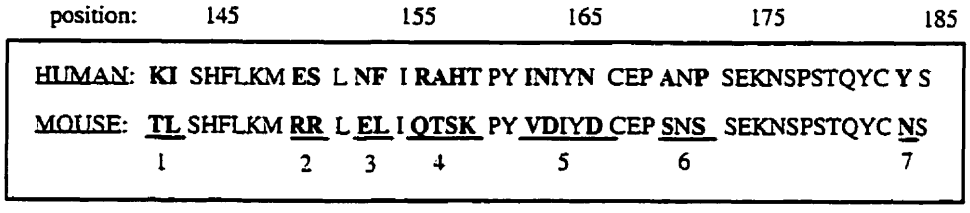

FIGURE V.4. CD20 human to murine extracellular domain mutants. The mutations which were used for the murinization of the human sequence are numbered, underlined and highlighted.

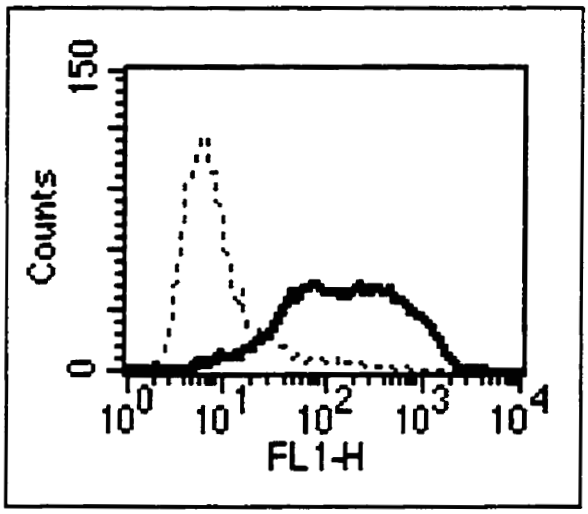

FIGURE V.5. FACScan profiles showing expression of CD20 on transfected HEK 293 cells. Cells transfected with empty vector (dashed line) or with CD20 cDNA in pCDM8 (bold line) were tested for the expression of CD20 by indirect immunofluorescence 2 days post-transfection.

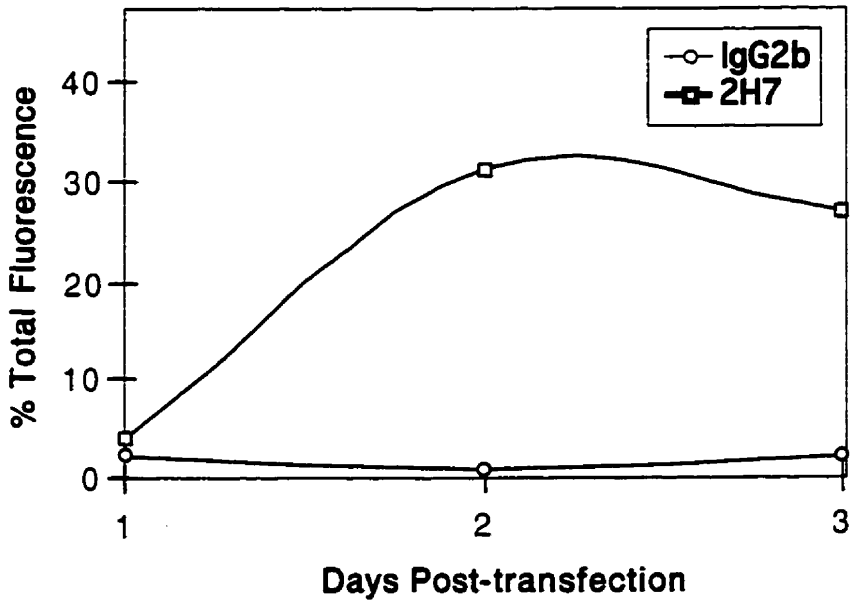

FIGURE V.6. CD20 expression maximal 2 to 3 days after transient transfection into HEK 293 cells. HEK 293 cell samples (~50% confluent) were transfected with 5 μg wild type CD20 cDNA by calcium phosphate method. CD20 expression 1, 2 or 3 days post-transfection was monitored by immunofluorescence using 2H7 anti-CD20 mAb or isotype control and FITC-labelled secondary mAb. (n=1)

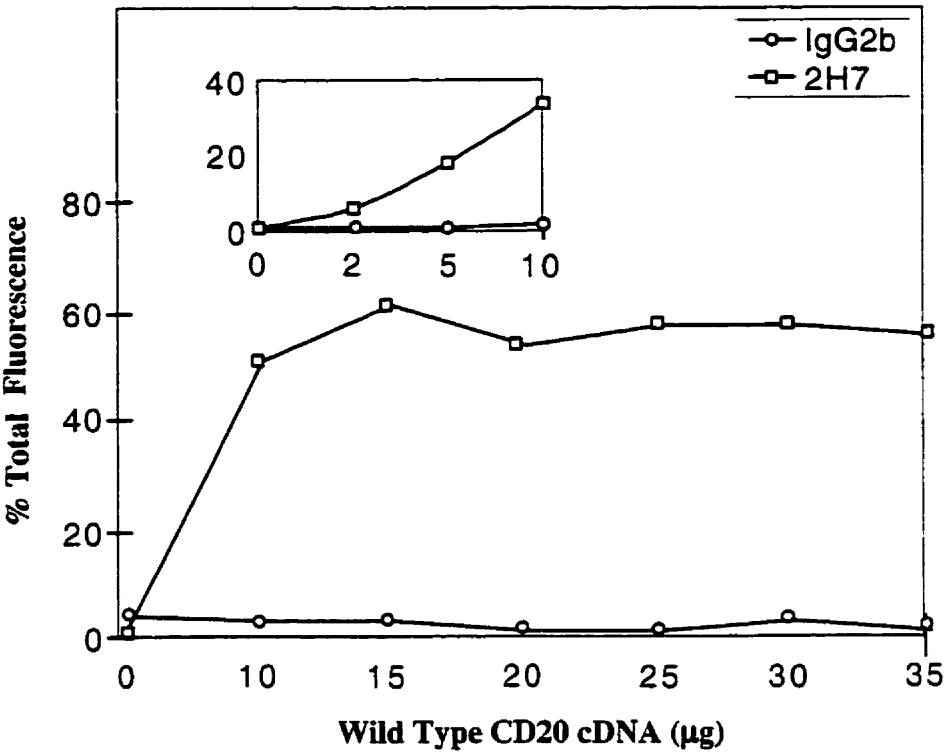

FIGURE V.7. Expression of CD20 transiently transfected into HEK 293 cells is maximal at 15 µg. Varying amounts of wild type CD20 cDNA in the expression vector pCDM8 was transfected into HEK 293 cells at ~50% confluence. Expression was monitored by FACs analysis 2 days post-transfection. *inset* Expression varied with minor changes up to 15 µg DNA transfected.

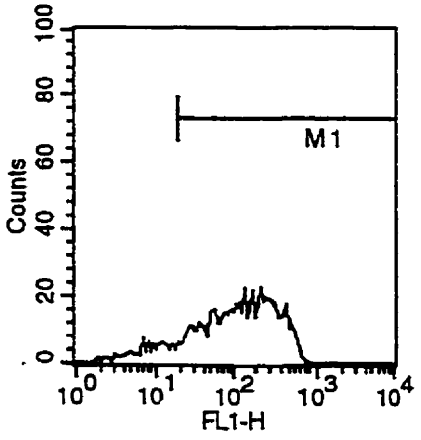

A

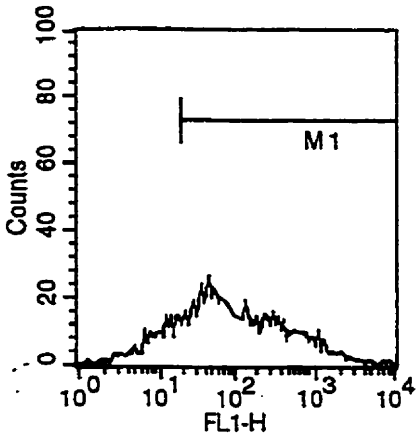

B

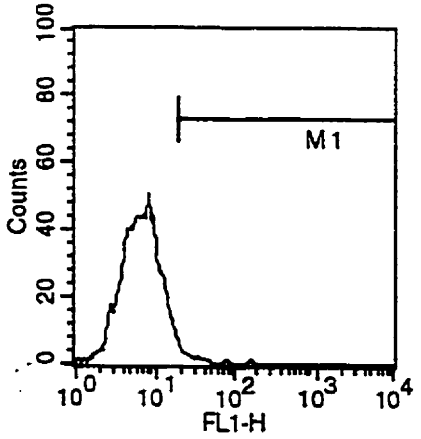

C

Fluorescence Values of 2H7 Binding

	% M1 Gate	Mean	Median
WT	90	151	112
Mutant 2	83	195	62
Mutant 6	1	7	7

D

FIGURE V.8. Example of raw FACscan data of anti-CD20 mAb binding to several constructs. Binding of 2H7 anti-CD20 mAb to constructs transiently expressed on HEK 293 cells as monitored by FACs analysis. *A*. Wild type CD20, *B*. Mutant 2, and *C*. Mutant 6. *D*. Various fluorescence parameters representing binding of 2H7 to each of the constructs is shown. Only the median value reflects the visible shift in the binding profile.

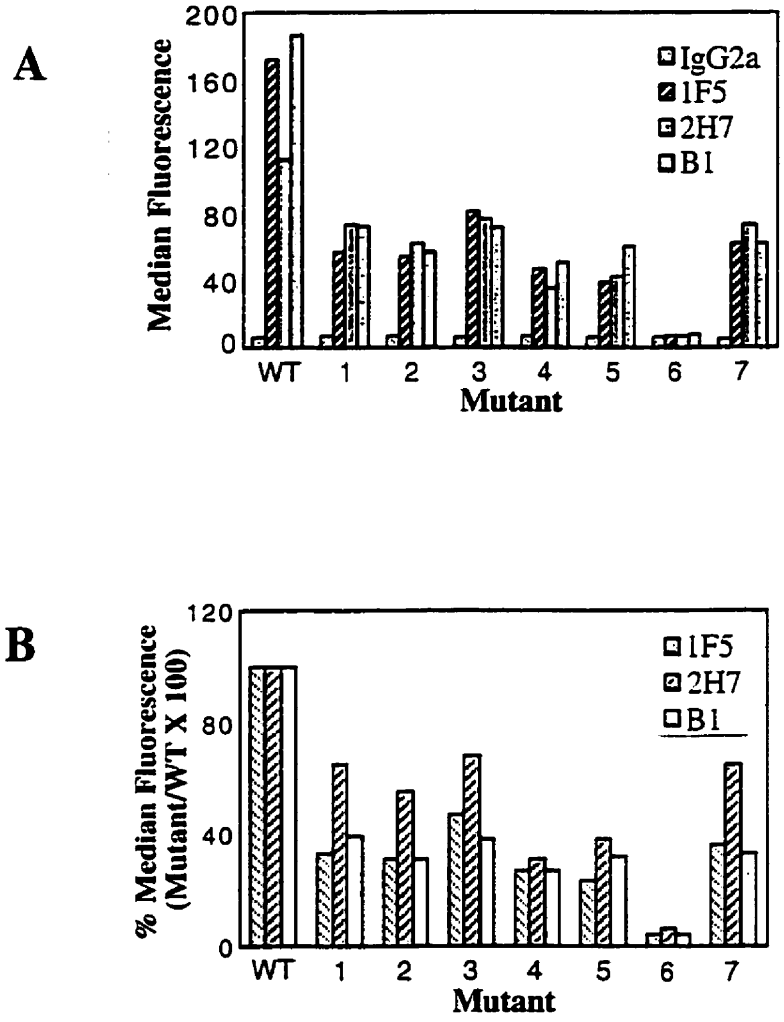

FIGURE V.9. Monoclonal Ab binding to CD20 human to murine extracellular domain mutants. Anti-human CD20 mAb binding to human/murine mutants expressed in HEK 293 cells was monitored by FACs analysis. *A.* The upper panel depicts raw median fluorescence values. *B.* The lower panel shows the same data as percent binding compared to wild type.

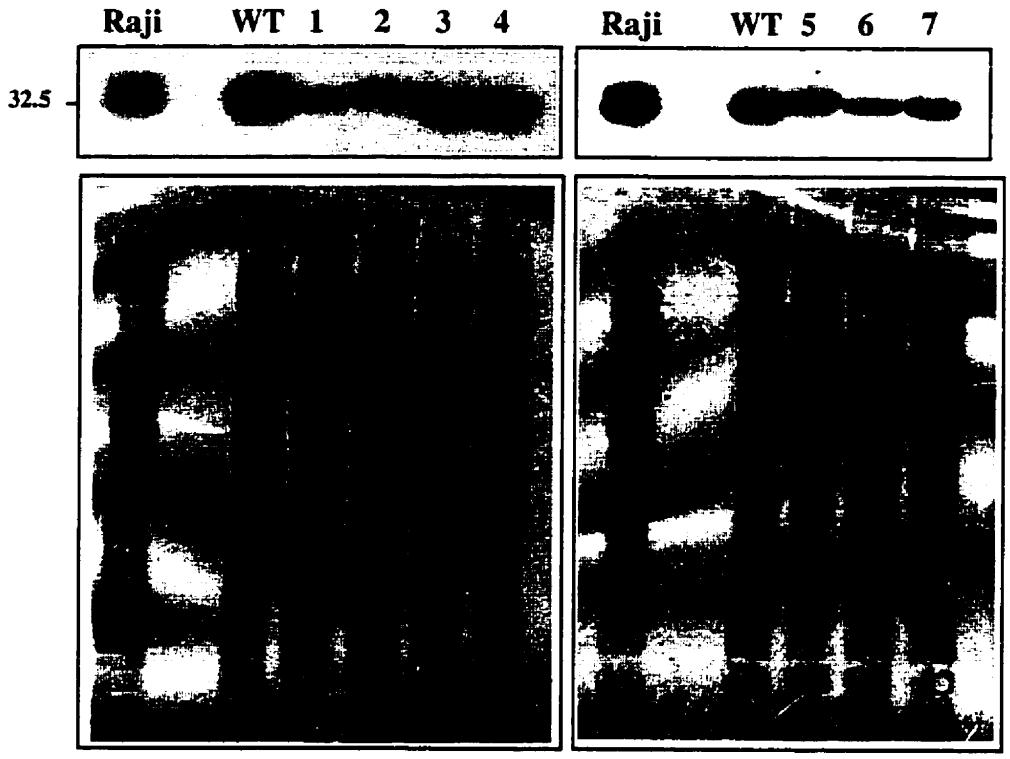

FIGURE V.10. Transiently transfected HEK 293 cells expressing varying levels of wild type and mutant CD20. Lysates from HEK 293 cells transiently transfected with either wild type (WT) or mutant CD20 (Mutants 1-7) (36 μg /sample) were separated on SDS-PAGE and CD20 expression monitored by immunoblotting with anti-CD20N antibody. Protein loading was confirmed by Coomassie Blue staining.

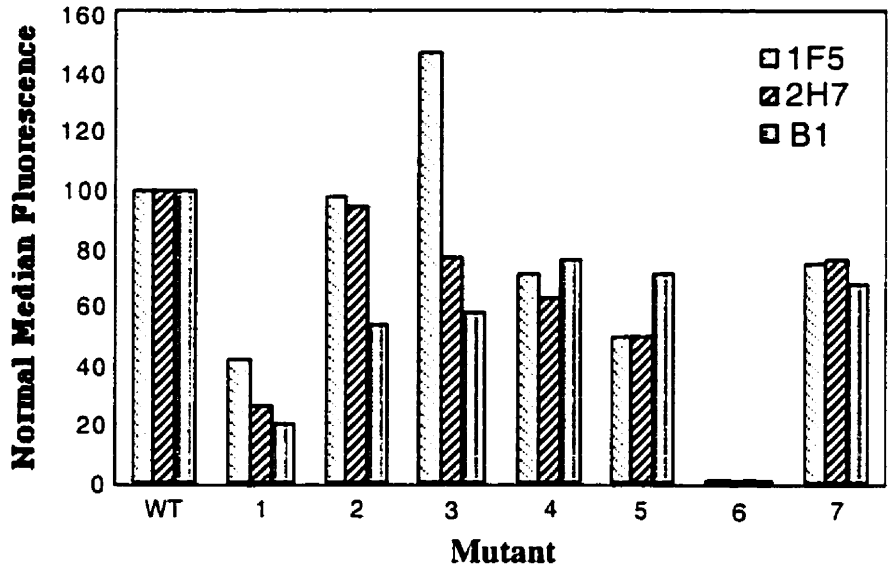

FIGURE V.11. Binding of three anti-CD20 mAbs was abolished by Mutant 6 (ANP/SNS). Anti-CD20 mAb binding to wild type human CD20 (WT) and human/murine Mutants 1-7 expressed in HEK 293 cells was monitored by FACs analysis. Raw total median fluorescence values were normalized for expression. (n=3)

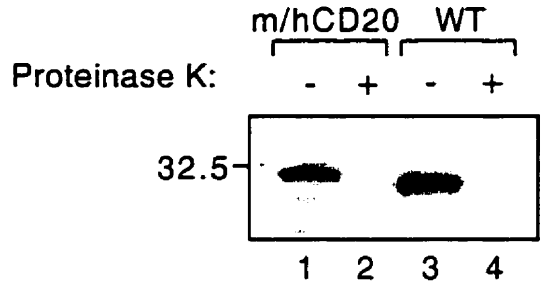

FIGURE V.12. Mouse/human chimera CD20 is expressed on the surface of transfected cells. HEK 293 cells transfected with either mouse/human chimera CD20 (m/hCD20; lanes 1 and 2) or wild type CD20 (WT; lanes 3 and 4) were either untreated or digested with proteinase K before lysis. Samples were analysed by SDS-PAGE and immunoblot with anti-CD20N antibody. In the digested samples,the 33 kDa CD20 band disappeared and a fragment of ~15 kDa corresponding to the N-terminal region was detected (not shown).

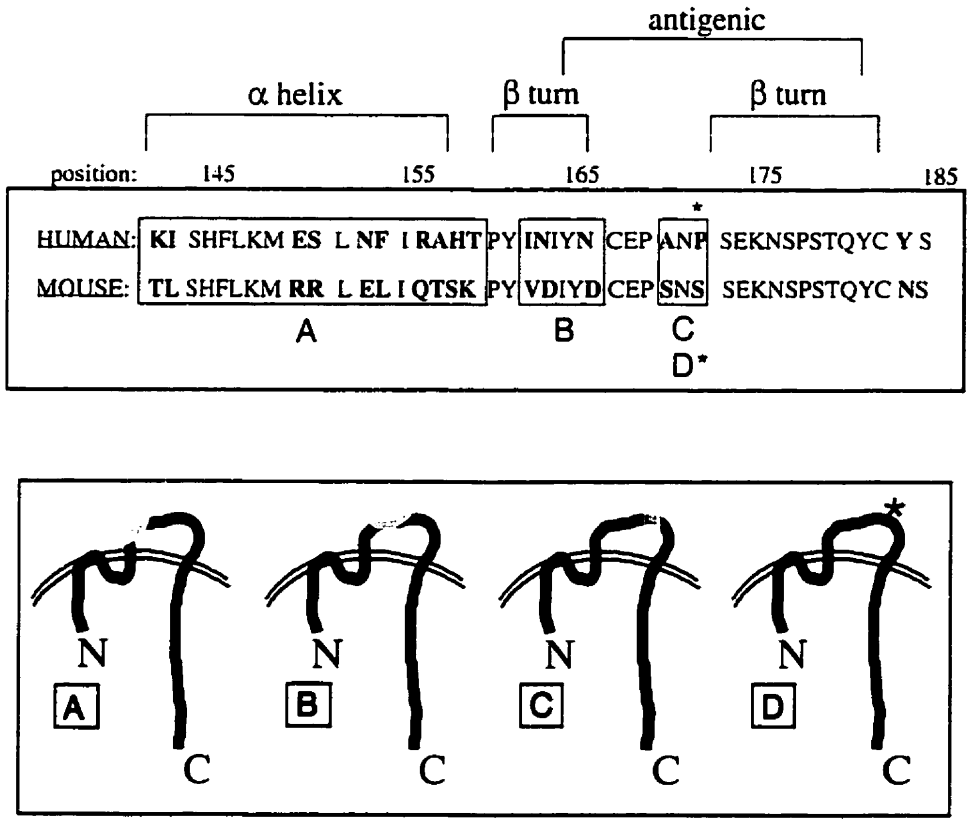

FIGURE V.13. Mouse to human CD20 extracellular domain mutants. Initially, the human CD20 extracellular domain was converted entirely to murine. Mutations for the humanization of the murine sequence are alphabetized, underlined and highlighted. Stretches of residues having a predicted secondary structure and antigenicity are indicated.

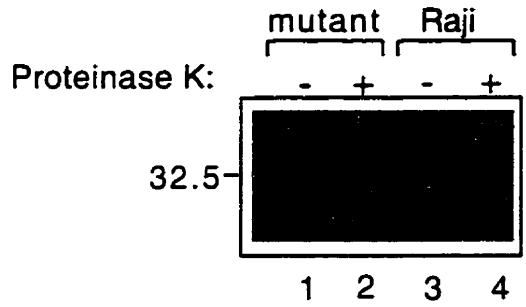

FIGURE V.14. CD20 mutants are expressed on the surface of transfected cells. HEK 293 cells transfected with either mutant CD20 (Mutant C; lanes 1 and 2) or wild type CD20 (Raji; lanes 3 and 4) were either untreated or digested with proteinase K before lysis. Samples were analysed by SDS-PAGE and immnoblot with anti-CD20N antibody. In the digested samples,the 33 kDa CD20 band disappeared and a fragment of ~15 kDa corresponding to the N-terminal region was detected (not shown). Similar data was obtained for Mutants A, B and D.

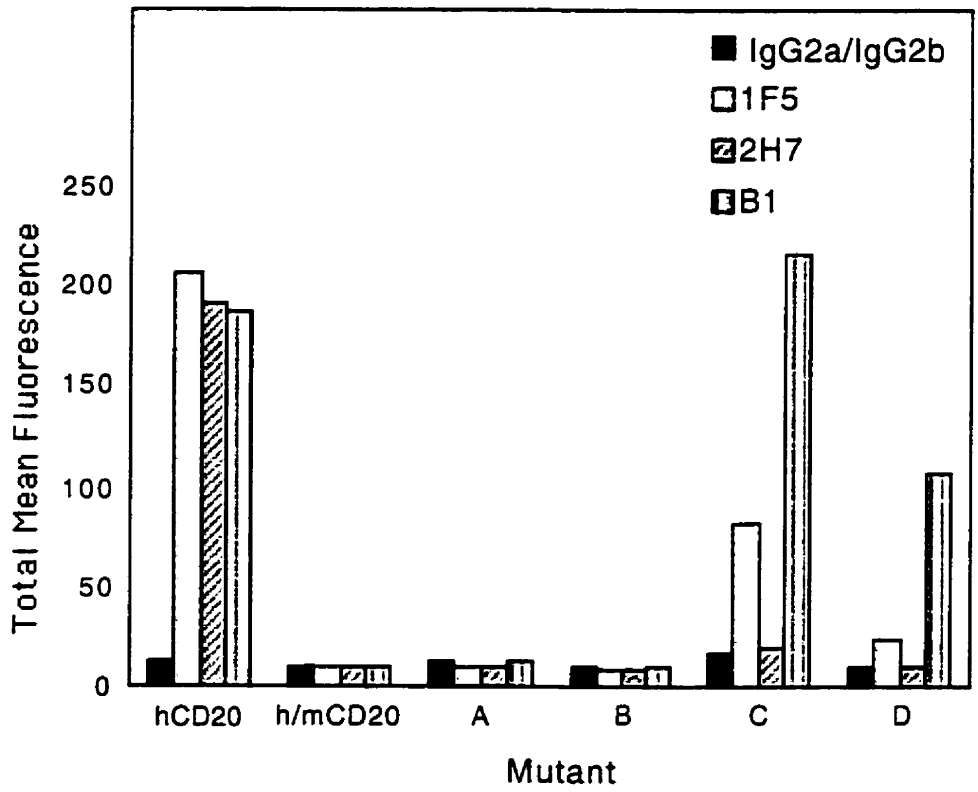

Figure V.15. Mutant C (SNS/ANP) recovers binding of only one anti-CD20 mAb . Anti-human CD20 mAb binding to murine/human mutants expressed in HEK 293 cells was monitored by FACs analysis (n=3).

VI. DISCUSSION AND FUTURE DIRECTIONS

A. Overview

In this study, I partially identified the specific amino acid residues which comprise the epitopes of three anti-CD20 mAbs. The epitope mapping results demonstrated that contrary to the cross-blocking experiments, B1 and 2H7 mAbs recognize unique epitopes. The epitope of B1 overlaps that of 1F5. These epitopes are on molecules in a ~200 kDa complex comprised primarily of CD20 with a ~45 kDa minor component. Prior to conducting the epitope mapping studies, the predicted CD20 membrane orientation was confirmed.

Confirmation of CD20 membrane orientation and its presence in a ~200 kDa complex is consistent with the suggestion that CD20 is a calcium channel (95). Other channels are also homooligomeric complexes comprised of molecules which span the membrane four times (96, 97). Although CD20 is homooligomeric, its association with signaling molecules suggests that it is likely a signaling component of a receptor or may be a receptor itself.

B. The CD20 Complex

1. Evidence

The ~200 kDa CD20 complex was identified in digitonin lysates, but was not maintained in Triton X-100. Although possible, it is unlikely that the observed CD20 complex is an artefact of the detergent. Several experiments in which digitonin has been

utilized to identify the components of transmembrane complexes have clearly demonstrated that digitonin is a more stringent detergent than other mild detergents such as Brij97 or CHAPS since fewer molecules co-precipitate in digitonin (124, 123). As well, digitonin stabilizes hydrophobic interactions which would otherwise be labile in other harsh detergents (119, 118). It is this property of digitonin which had allowed for the identification of the association of the BCR with Igα and Igβ (120). The components of the B cell receptor complex could only be successfully kept intact and thereby identified using digitonin (120) and β octyl glucoside (121).

Use of the flow cytometric electron transfer method, which is used to demonstrate the proximity of certain cell surface molecules, had demonstrated that only a single CD20 molecule was present in the MHCII-tetraspan complex examined. In this method, energy transfer between fluorescently labeled mAbs was monitored (55). Since anti-CD20 mAbs may recognize epitopes on adjacent molecules, steric hindrance may have prevented mAb binding to each molecule in the complex thereby affecting the interpretation of the results.

Previous chemical cross-linking studies have shown that CD20 appears to exist as a monomer, dimer, and tetramer (95). The absence of CD20 monomers and dimers in digitonin suggests that the CD20 complex observed in digitonin is likely comprised of a dimer of CD20 dimers in addition to the ~45 kDa unidentified protein. This is very likely since CD20 was observed to form dimers *in vitro* under non-reducing conditions (Figure

IV. 3). The presence of a ~142 kDa CD20 tetramer and additional molecules including the unidentified ~45 kDa protein would account for the size of the complex.

2. Additional Experiments

2.1 Confirmation of Complex Size

Despite the likelihood that the velocity gradient experiments are correct in demonstrating that CD20 exists in a ~200 kDa complex, other experiments will have to be conducted to confirm the size of the complex and to identify its components. The size of native proteins has been successfully determined using non-denaturing conditions. This method could be used to determine the size of the CD20 complex. Unfortunately, such an experiment would still not eliminate the potential affect of the detergent.

2.2 Identifying the Components of the Complex

Identifying the number of CD20 molecules present in the complex would aid in confirming the proportion of the complex comprised of CD20. If it appeared that four CD20 molecules were present, then the predicted molecular weight of the complex would be feasible. The number of CD20 molecules present in the complex could be determined by co-transfection of decreasing amounts of epitope-tagged CD20 construct and wild type CD20 using the already established transfection system. The CD20 complex could be precipitated using antibody specific for the epitope-tag and the ratio of epitope-tagged CD20 to wild type CD20 determined by SDS-PAGE and Western blot analysis using an antibody which recognized both forms of CD20. With decreasing amount of epitope-tagged construct expressed, the epitope-tagged construct would be diluted out until there

would be only a single construct per complex thereby allowing for the quantity of CD20 molecules present in the complex to be identified.

Identifying the ~45 kDa component of the complex will be very important in confirming the size of the complex as well as in determining the specific role of CD20. Co-precipitation experiments using antibody against candidate proteins could be conducted. Candidate proteins would include the transmembrane proteins of 40 to 48 kDa in size such as CD23 (45 kDa), CD32 (40 kDa), and CD40 (48 kDa). Preliminary experiments have demonstrated this approach to be problematic since CD20 also co-precipitated with some of the isotype controls. If these results are correct, however, the ~45 kDa protein may be the FcγR (CD32). This result would not be unexpected since CD20 is related to FcεRIβ. Alternatively, co-precipitation using anti-CD20N antibody and subsequent Western blot for candidate proteins could also be conducted. Unfortunately, blotting antibodies for most candidate proteins do not exist.

Although the association of the ~45 kDa protein with CD20 in digitonin suggests that the unidentified protein is hydrophobic in nature, suggesting it is a transmembrane protein, there is a possibility this protein does not have an extracellular component as the cell surface biotinylation experiments suggested (Figure IV. 6). Another approach would be to sequence the product and determine its identity by comparison with the protein sequence database. Since biotin labeling resulted in the precipitation of numerous non-specific proteins, immunoprecipitation of CD20 from [S^{35}]-methionine metabolically labeled or unlabelled lysate could reduce the quantity of non-specific proteins and may

allow for the appropriate band to be distinguished and identified using mass spectrometry or amino acid analysis.

2.3 Requirements for Complex Formation

Analysis of the requirement of the cytoplasmic domains for CD20 complex formation suggested that the membrane distal portion of the C-terminal region was not required, while the N-terminal and membrane proximal C-terminal regions may be required but to a minor extent. This result indicates that although the membrane proximal residues 219-252 in the C-terminal region are important for CD20 redistribution, they are likely not required for complex formation. To examine whether other domains are important in CD20 complex formation, transmembrane and extracellular domain mutants could be examined. The ANP/SNS mutant which abolished binding of all mAbs tested in the negative binding strategy could be examined for its involvement in complex formation. It is possible that the ANP/SNS mutation disrupted the complex thereby eliminating the epitopes of the anti-CD20 mAbs.

As well, since digitonin maintains hydrophobic interactions, it is very possible that the integrity of the complex is dependent upon CD20 transmembrane domains. Testing this premise would be difficult in that the transmembrane domains of CD20 could not be simply swapped with that of, for example, any of the tetraspan family members since most of these molecules are involved in heteroligomers (55, 123, 124, 141). Each CD20 transmembrane domain could be swapped stepwise with a transmembrane domain of a molecule known to be monomeric in nature. However, since a point mutation in the

third transmembrane domain completely prevented cell surface expression of CD20 (71), it is unlikely that major alterations could be made without affecting CD20 expression.

It is possible that an additional reason for the inability of anti-human CD20 extracellular domain mAbs to recognize murine CD20 is that it may not be able to form complexes. The human CD20 containing the murine extracellular domain could be tested for its ability to form complexes. Also, despite the high degree of homology between the human and murine transmembrane domains, swapping the murine transmembrane domains for those in human CD20 may have an affect on complex formation.

C. CD20 Epitope Mapping

1. Results and Implications

Although the intent of this study was to completely identify the epitopes of the three anti-human CD20 mAbs tested, the epitopes were only partially mapped. Importantly, however, the epitope mapping results demonstrated that contrary to the cross-blocking experiments (142), B1 and 2H7 mAbs recognize unique epitopes. As well, the epitope of B1 overlaps that of 1F5. The results from the positive binding strategy suggested that the B1 epitope was completely dependent upon the residues ANP, while the 1F5 epitope was also partially comprised of ANP and additional residues dependent upon the secondary structure conferred by these residues. The epitope of 2H7 does not include the ANP residues but is dependent upon the secondary structure conferred by these residues for recognition of its epitope. These results were consistent with the

various biochemical and biological responses induced by ligation of the different antibodies.

1.1 CD20 Redistribution

The CD20 complex is excluded from lipid rafts in the plasma membrane prior to stimulation (72). Ligation of its extracellular domain results in CD20 redistribution to these lipid rafts with the degree depending upon the antibody. Differential distribution is likely the result of the recognition of different epitopes. Ligation of unidentified residues by 2H7 initiates the greatest degree of redistribution (95%). B1 which recognizes ANP causes 5% redistibution, while ligation of 1F5 to ANP and other unidentified residues causes redistribution of 50%, a value between that of 2H7 and B1. It appears that ligation of the ANP residues is less conducive to redistribution, while ligation of the unidentified residues enhance redistribution.

The membrane proximal residues 219-252 in the CD20 C-terminal region are required for the redistribution of CD20 (90). It is possible that ligation of the CD20 extracellular domain causes a conformational change in this stretch of amino acids resulting in protein-protein interactions, signaling events and, in turn, its redistribution. Degree of conformational change is likely dependent upon the ligating mAb. Since 2H7 ligation of CD20 initiates the greatest degree of redistribution, it is likely that the conformational change induced in this stretch of residues is most profound with 2H7 treatment. Changes in the conformation and/or protein-protein associations could be examined by intracellular staining using anti-CD20N or anti-CD20C antibodies of cells before and after CD20 stimulation. The disappearance of epitopes recognized by either antibodies could indicate

a conformational change in the epitope and possibly the sequestration of the epitope resulting from protein-protein interaction.

1.2 B1

Based on the epitope mapping results and the functional studies of CD20 reported in the literature, it appears that the CD20 conformation is dependent upon the stage of B cell activation. In addition to its ability to cause only ~5% CD20 redistribution, B1 binding to its epitope (ANP) in the CD20 extracellular domain initiates a series of signaling events which are somewhat distinct from that of 1F5 and 2H7.

B1 ligation of CD20 inhibits B cell proliferation as does 2H7 (66, 101), but uniquely results in B cell homotypic aggregation. The phenotype associated with B1 ligation of CD20 is similar to that induced by CD81 or CD19 ligation. As mentioned previously, CD81 is a tetraspan molecule which acts as the bridge between the tetraspan web and the BCR CD19 co-receptor complex (124). The tetraspan web is comprised of other tetraspans, β1 integrins and MHCII. The tetraspan and non-tetraspan members of the tetraspan web are identified by their ability to induce similar effects including homotypic aggregation. It therefore appears that B1 ligation of CD20 may somehow enhance its association with the tetraspan web. Indeed, flow cytometric energy transfer experiments have suggested that CD20 is in close physical proximity to MHCII and several tetraspan molecules including CD81 (55). A structural and functional association between CD20 and MHCII has been demonstrated in CHAPS (56). It is possible this association mimics one induced by B1 ligation of CD20 since CHAPS is a non-stringent

detergent thereby allowing for the co-precipitation of a greater quantity of associated molecules. The B1 induced association of CD20 with the tetraspan web implies that the conformation of CD20 and subsequent signaling events somehow mimic those that occur just prior to and including B cell heterotypic aggregation during co-stimulation by T cells.

1.3 1F5

Binding of 1F5 to its epitope comprised of ANP and additional unknown residues results in its unique ability to activate resting B cells. The series of events initiated by 1F5 appear to mimic the effects of IL-4 on B cells. As mentioned previously, 1F5 induces resting B cells to enlarge and then enter G1 phase of the cell cycle accompanied by increased levels of MHCII expression (62, 64, 101). After an additional co-stimulatory signal, the B cells start to proliferate. IL-4 also causes cell enlargement and increased expression of MHCII, but does not induce cells to enter G1 phase (143, 144). IL-4 treatment of B cells results in a conformational change which makes the CD20 epitope recognized by L27 mAb inaccessible (58). This conformation change is reversed by CD40 stimulation. 1F5 ligation of CD20 may mimic the conformational change induced by IL-4 during the initial phase of B cell activation.

1.4 2H7

The conformational changes induced by 2H7 are most conducive to CD20 redistribution to lipid rafts. Virtually all of the 2H7 stimulated CD20 localizes to Triton X-100 insoluble component of lipid rafts in which src family kinases have been shown to localize. Oddly, the small population of CD20 remaining in the Triton X-100 soluble fraction precipitates the greatest degree of associated src family kinases lyn, lck, and fyn

as well as the unidentified p75/80 (71). Recently, studies examining the regulation of the src family kinases lck and fyn in T cells has suggested that these molecules are localized in a core microdomain and regulated by transmembrane proteins in the periphery of the lipid raft (145). The same could be the case with 2H7 ligated CD20 in that the majority of molecules may localize to the core of the lipid raft and the remainder are in the periphery. CD20 redistribution may enhance its accessibility to the signaling proteins present in the lipid rafts. As a result, the molecules being precipitated from 2H7 stimulated B cell lysate actually represent the molecules which are associated with CD20 on the periphery of the lipid raft. Since 2H7 ligation enhances redistribution to lipid rafts where CD20 may modulate signals of other transmembrane proteins present, mapping the residues important in inducing redistribution would greatly aid in our understanding of the role of CD20.

1..5 Significance

The various effects of the different anti-CD20 mAbs appear to suggest contrary roles for CD20. 1F5 causes B cell activation, while 2H7 initiates changes potentially involving B cell modulation. 1F5 could be inducing a CD20 conformational change required during activation. The conformational changes induced by 2H7 may be required for modulation of the B cell by CD20.

2. Additional Experiments

2.1 Completing the Epitope Map of 1F5 and 2H7

Further epitope mapping studies should be conducted to identify the residues of 1F5 and 2H7. Since the constructs used for the studies outlined here were not sufficient for identifying the residues recognized by these two mAbs, additional constructs will have to be developed to elucidate their epitopes. The results demonstrate that the secondary structure of the CD20 extracellular domain is vital for mAb binding. Because the negative binding strategy demonstrated that the ANP residues were required for binding by all mAbs, these residues should be included in all subsequent constructs in a positive binding strategy. The ANP residues would be mutated in conjunction with the other non-homologous residues stepwise. Initially, since it appears that the β turn formed by the human INIYN stretch of residues may also be indirectly involved in the epitope in that it also provides secondary structure, INIYN would be converted with ANP in m/hCD20. The other non-homologous residues would be converted individually or in subsets stepwise based on the results of secondary structure analysis so that the mutations would still provide the secondary structure necessary to recover mAb binding.

If discontinuous residues are involved in epitope formation, then the epitope could be appropriately divided onto two constructs to determine whether the epitope was on adjacent molecules. The two constructs could be co-transfected and mAb binding monitored. Enhanced binding would suggest the epitope was on adjacent molecules and could aid in identifying the organization of the CD20 molecules in the complex.

2.2 Mapping the Epitopes of Additional mAbs

The constructs used in the positive binding strategy as well as those suggested for future experiments could also be used in identifying the epitopes of other anti-CD20 mAbs. The epitope of R21 mAb used in identifying the association of CD20 with CD40 and MHCII would be of interest since it appears to recognize a continuous epitope of the CD20 extracellular domain. Mapping the epitope of L27 mAb could be of particular importance since it is the only epitope known which disappears with a physiological stimulus, which is the IL-4 treatment of B cells. As well, mapping the epitopes of Rituxim™ might provide insight into its efficacy in treating non-Hodgkin's lymphoma and AARP's.

2.3 CD20 Complex Dynamics

Once the epitopes are identified, it will be of interest to determine whether the various mAbs cause redistribution of various populations of the CD20 complex to lipid rafts. For instance, since it is likely that B1 recognizes an epitope on a single CD20 molecule, it may be feasible that its ligation of CD20 may cause the dissociation of the complex. As well, if 2H7 does recognize a discontinuous epitope on adjacent molecules, then ligation of the complex could cause further aggregation of CD20 within the lipid rafts. In order to pursue such studies, intact B cells would have to be stimulated with the individual anti-CD20 mAbs covalently conjugated to sepharose beads, the cells lysed in digitonin and either the digitonin soluble fraction or the solubilized digitonin insoluble fraction treated with SDS separated by velocity gradient centrifugation to determine complex molecular weight.

D. Significance

Here, I have demonstrated that the three anti-CD20 mAbs tested recognize different epitopes on a ~200 kDa CD20 complex. The recognition of unique epitopes by the various antibodies is consistent with the different biochemical changes and biological responses induced upon ligation. For example, the ability of the various anti-CD20 mAbs to cause redistribution of CD20 to lipid rafts is mAb and, thereby, epitope dependent.

Recently in our laboratory, we observed that the unusual property of redistribution is shared by the BCR. Upon stimulation, a sub-population of BCR also redistributes to lipid rafts where signaling events are detected. The redistribution of the BCR may be associated with the down-regulation of the B cell response since experiments have shown that FcγRIIB1 (CD32) and BCR co-localize to caps on the cell surface. Since CD20 is involved in regulating B cell activation, the redistribution of these proteins to lipid rafts likely has functional significance. The homology of CD20 with FcεRIβ and its signaling properties may even suggest that it is a component of the FcγRII complex. Modulation of B cell receptor function by CD20 is currently being investigated in our laboratory.

REFERENCES

1. Pleiman CM, D'Ambrosio D, Cambier JC. The B-cell antigen receptor complex: structure and signal transduction. Immunol Today 1994;15(9):393-9.

2. Gold MR, Matsuuchi L. Signal transduction by the antigen receptors of B and T lymphocytes. Int Rev Cytol 1995;157:181-276.

3. Song H, Nie X, Basu S, Cerny J. Antibody feedback and somatic mutation in B cells: regulation of mutation by immune complexes with IgG antibody. Immunol Rev 1998;162:211-8.

4. Tarlinton D. Germinal Centers: Form and Function. Current Opinion in Immunology 1999;10:245-251.

5. Liu Y, and C. Arpin. Germinal Center Development. Immunological Reviews 1997;156:111-126.

6. Camacho SA, Kosco-Vilbois MH, Berek C. The dynamic structure of the germinal center. Immunol Today 1998;19(11):511-4.

7. Kosco-Vilbois MH, Zentgraf H, Gerdes J, Bonnefoy JY. To 'B' or not to 'B' a germinal center? Immunol Today 1997;18(5):225-30.

8. Arpin C, Dechanet J, Van Kooten C, et al. Generation of memory B cells and plasma cells in vitro. Science 1995;268(5211):720-2.

9. Lefkowith JB, Gilkeson GS. Nephritogenic autoantibodies in lupus: current concepts and continuing controversies. Arthritis Rheum 1996;39(6):894-903.

10. Drake CG, Kotzin BL. Genetic and immunological mechanisms in the pathogenesis of systemic lupus erythematosus. Curr Opin Immunol 1992;4(6):733-40.

11. Reth M. Antigen receptor tail clue [letter]. Nature 1989;338(6214):383-4.

12. Cambier JC, Pleiman CM, Clark MR. Signal transduction by the B cell antigen receptor and its coreceptors. Annu Rev Immunol 1994;12:457-86.

13. Kurosaki T. Genetic analysis of B cell antigen receptor signaling. Annu Rev Immunol 1999;17:555-92.

14. Campbell KS. Signal Transduction from the B cell antigen-receptor. Current Opinion in Immunology 1999;11:256-264.

15. Takata M, Kurosaki T. A role for Bruton's tyrosine kinase in B cell antigen receptor-mediated activation of phospholipase C-gamma 2. J Exp Med 1996;184(1):31-40.

16. Baixeras E, Kroemer G, Cuende E, et al. Signal transduction pathways involved in B-cell induction. Immunol Rev 1993;132:5-47.

17. Jiang A, Craxton A, Kurosaki T, Clark EA. Different protein tyrosine kinases are required for B cell antigen receptor-mediated activation of extracellular signal-regulated kinase, c-Jun NH2-terminal kinase 1, and p38 mitogen-activated protein kinase. J Exp Med 1998;188(7):1297-306.

18. Hashimoto A, Okada H, Jiang A, et al. Involvement of guanosine triphosphatases and phospholipase C-gamma2 in extracellular signal-regulated kinase, c-Jun NH2-terminal kinase, and p38 mitogen-activated protein kinase activation by the B cell antigen receptor. J Exp Med 1998;188(7):1287-95.

19. Yamamoto T, Yamanashi Y, Toyoshima K. Association of Src-family kinase Lyn with B-cell antigen receptor. Immunol Rev 1993;132:187-206.

20. Vanhaesebroeck B, Leevers SJ, Panayotou G, Waterfield MD. Phosphoinositide 3-kinases: a conserved family of signal transducers. Trends Biochem Sci 1997;22(7):267-72.

21. Fu C, Turck CW, Kurosaki T, Chan AC. BLNK: a central linker protein in B cell activation. Immunity 1998;9(1):93-103.

22. Wienands J, Schweikert J, Wollscheid B, Jumaa H, Nielsen PJ, Reth M. SLP-65: a new signaling component in B lymphocytes which requires expression of the antigen receptor for phosphorylation. J Exp Med 1998;188(4):791-5.

23. Callard RE, Matthews DJ, Hibbert L. IL-4 and IL-13 receptors: are they one and the same? Immunol Today 1996;17(3):108-10.

24. Tsubata T. Co-receptors on B lymphocytes. Curr Opin Immunol 1999;11(3):249-55.

25. Tedder TF, Inaoki M, Sato S. The CD19-CD21 complex regulates signal transduction thresholds governing humoral immunity and autoimmunity. Immunity 1997;6(2):107-18.

26. Carter RH, Doody GM, Bolen JB, Fearon DT. Membrane IgM-induced tyrosine phosphorylation of CD19 requires a CD19 domain that mediates association with components of the B cell antigen receptor complex. J Immunol 1997;158(7):3062-9.

27. Buhl AM, Cambier JC. Co-receptor and accessory regulation of B-cell antigen receptor signal transduction. Immunol Rev 1997;160:127-38.

28. Weiss A, Littman DR. Signal transduction by lymphocyte antigen receptors. Cell 1994;76(2):263-74.

29. Tedder TF, Zhou LJ, Engel P. The CD19/CD21 signal transduction complex of B lymphocytes. Immunol Today 1994;15(9):437-42.

30. O'Rourke LM, Tooze R, Turner M, et al. CD19 as a membrane-anchored adaptor protein of B lymphocytes: costimulation of lipid and protein kinases by recruitment of Vav. Immunity 1998;8(5):635-45.

31. Uckun FM, Burkhardt AL, Jarvis L, et al. Signal transduction through the CD19 receptor during discrete developmental stages of human B-cell ontogeny. J. Biol. Chem. 1993;268:21172-21184.

32. Sato S, Jansen PJ, Tedder TF. CD19 and CD22 expression reciprocally regulates tyrosine phosphorylation of Vav protein during B lymphocyte signaling. Proc Natl Acad Sci U S A 1997;94(24):13158-62.

33. Rickert RC, Rajewsky K, Roes J. Impairment of T-cell-dependent B-cell responses and B-1 cell development in CD19-deficient mice. Nature 1995;376(6538):352-5.

34. Tuscano J, Engel P, Tedder TF, Kehrl JH. Engagement of the adhesion receptor CD22 triggers a potent stimulatory signal for B cells and blocking CD22/CD22L interactions impairs T-cell proliferation. Blood 1996;87(11):4723-30.

35. Tooze RM, Doody GM, Fearon DT. Counterregulation by the coreceptors CD19 and CD22 of MAP kinase activation by membrane immunoglobulin. Immunity 1997;7(1):59-67.

36. O'Keefe TL, Williams GT, Davies SL, Neuberger MS. Hyperresponsive B cells in CD22-deficient mice. Science 1996;274(5288):798-801.

37. Hibbs ML, Tarlinton DM, Armes J, et al. Multiple defects in the immune system of Lyn-deficient mice, culminating in autoimmune disease. Cell 1995;83(2):301-11.

38. Takata M, Sabe H, Hata A, et al. Tyrosine kinases Lyn and Syk regulate B cell receptor-coupled Ca2+ mobilization through distinct pathways. Embo J 1994;13(6):1341-9.

39. Cyster JG, Goodnow CC. Protein tyrosine phosphatase 1C negatively regulates antigen receptor signaling in B lymphocytes and determines thresholds for negative selection. Immunity 1995;2(1):13-24.

40. Siminovitch KA, Neel BG. Regulation of B cell signal transduction by SH2-containing protein- tyrosine phosphatases. Semin Immunol 1998;10(4):329-47.

41. Fujimoto M, Poe JC, Jansen PJ, Sato S, Tedder TF. CD19 amplifies B lymphocyte signal transduction by regulating Src- family protein tyrosine kinase activation. J Immunol 1999;162(12):7088-94.

42. Coggeshall KM. Inhibitory signaling by B cell Fc gamma RIIb. Curr Opin Immunol 1998;10(3):306-12.

43. Minskoff SA, Matter K, Mellman I. Fc gamma RII-B1 regulates the presentation of B cell receptor-bound antigens. J Immunol 1998;161(5):2079-83.

44. Amigorena S, Bonnerot C, Drake JR, et al. Cytoplasmic domain heterogeneity and functions of IgG Fc receptors in B lymphocytes. Science 1992;256(5065):1808-12.

45. Bewarder N, Weinrich V, Budde P, et al. In vivo and in vitro specificity of protein tyrosine kinases for immunoglobulin G receptor (FcgammaRII) phosphorylation. Mol Cell Biol 1996;16(9):4735-43.

46. Daeron M, Malbec O, Latour S, Espinosa E, Pina P, Fridman WH. Regulation of tyrosine-containing activation motif-dependent cell signalling by Fc gamma RII. Immunol Lett 1995;44(2-3):119-23.

47. Ono M, Bolland S, Tempst P, Ravetch JV. Role of the inositol phosphatase SHIP in negative regulation of the immune system by the receptor Fc(gamma)RIIB. Nature 1996;383(6597):263-6.

48. Sarkar S, Schlottmann K, Cooney D, Coggeshall KM. Negative signaling via FcgammaRIIB1 in B cells blocks phospholipase Cgamma2 tyrosine phosphorylation but not Syk or Lyn activation. J Biol Chem 1996;271(33):20182-6.

49. Hippen KL, Buhl AM, D'Ambrosio D, Nakamura K, Persin C, Cambier JC. Fc gammaRIIB1 inhibition of BCR-mediated phosphoinositide hydrolysis and Ca2+ mobilization is integrated by CD19 dephosphorylation. Immunity 1997;7(1):49-58.

50. Kiener PA, Lioubin MN, Rohrschneider LR, Ledbetter JA, Nadler SG, Diegel ML. Co-ligation of the antigen and Fc receptors gives rise to the selective modulation of intracellular signaling in B cells. Regulation of the association of phosphatidylinositol 3-kinase and inositol 5'- phosphatase with the antigen receptor complex. J Biol Chem 1997;272(6):3838-44.

51. Gottschalk AR, Joseph LJ, Quintans J. Fc gamma RII cross-linking inhibits anti-Ig-induced erg-1 and erg-2 expression in BCL1. J Immunol 1994;152(5):2115-22.

52. Tridandapani S, Chacko GW, Van Brocklyn JR, Coggeshall KM. Negative signaling in B cells causes reduced Ras activity by reducing Shc-Grb2 interactions. J Immunol 1997;158(3):1125-32.

53. Muta T, Kurosaki T, Misulovin Z, Sanchez M, Nussenzweig MC, Ravetch JV. A 13-amino-acid motif in the cytoplasmic domain of Fc gamma RIIB modulates B-cell receptor signalling [published erratum appears in Nature 1994 May 26;369(6478):340]. Nature 1994;368(6466):70-3.

54. Pearse RN, Kawabe T, Bolland S, Guinamard R, Kurosaki T, Ravetch JV. SHIP recruitment attenuates Fc gamma RIIB-induced B cell apoptosis. Immunity 1999;10(6):753-60.

55. Szollosi J, Horejsi, V., Bene, L., Angelisova, P. and Damjanovich, S.,. Supramolecular complexes of MHC class I, MHC class II, CD20, and tetraspan molecules (CD53, CD81, CD82) at the surface of the B cell line JY. The Journal of Immunology 1996;157:2939-2946.

56. Leveille C, R AL-D, Mourad W. CD20 is physically and functionally coupled to MHC class II and CD40 on human B cell lines. Eur J Immunol 1999;29(1):65-74.

57. Golay J, Cusmano G, Introna M. Independent regulation of c-myc, B-myb, and c-myb gene expression by inducers and inhibitors of proliferation in human B lymphocytes. J Immunol 1992;149(1):300-308.

58. Dancescu M, Wu C, Rubio M, Delespesse G, Sarfati M. IL-4 induces conformational change of CD20 antigen via a protein kinase C-independent pathway. Antagonistic effect of anti-CD40 monoclonal antibody. Journal of Immunology 1992;148(8):2411-6.

59. Rosenthal P, Rimm IJ, Umiel T, et al. Ontogeny of human hematopoietic cells: analysis utilizing monoclonal antibodies. Journal of Immunology 1983;131(1):232-7.

60. Tedder TF, Engel P. CD20: a regulator of cell-cycle progression of B lymphocytes. Immunology Today 1994;15(9):450-4.

61. Clark EA, Shu G, Ledbetter JA. Role of the Bp35 cell surface polypeptide in human B-cell activation. Proc. Natl. Acad. Sci. U.S.A. 1985;82:1766-1770.

62. Clark EA, Shu G. Activation of human B cell proliferation through surface Bp35 (CD20) polypeptides or immunoglobulin receptors. J Immunol 1987;138(3):720-725.

63. Golay JT, Clark EA, Beverley PC. The CD20 (Bp35) antigen is involved in activation of B cells from the G0 to the G1 phase of the cell cycle. Journal of Immunology 1985;135(6):3795-801.

64. Smeland E, Godal T, Ruud E, et al. The specific induction of myc protooncogene expression in normal human B cells is not a sufficient event for acquisition of competence to proliferate. Proc. Natl. Acad. Sci. U.S.A. 1985;82:6255-6259.

65. White MW, McConnell F, Shu GL, Morris DR, Clark EA. Activation of dense human tonsilar B cells. Induction of c-myc gene expression via two distinct signal transduction pathways. J. Immunol. 1991;146:846-853.

66. Tedder TF, Forsgren A, Boyd AW, Nadler LM, Schlossman SF. Antibodies reactive with the B1 molecule inhibit cell cycle progression but not activation of human B lymphocytes. Eur. J. Immunol. 1986;8:881-887.

67. Golay JT, Crawford DH. Pathways of human B-lymphocyte activation blocked by B-cell-specific monoclonal antibodies. Immunol. 1987;62:279.

68. Tedder TF, Boyd AW, Freedman AS, Nadler LM, Schlossman SF. The B cell surface molecule is functionally linked with B cell activation and differentiation. J. Immunol. 1985;135:973-.

69. Kansas GS, Tedder TF. Transmembrane signals generated through MHC class II, CD19, CD20, CD39, and CD40 antigens induce LFA-1-dependent and independent adhesion in human B cells through a tyrosine kinase-dependent pathway. Journal of Immunology 1991;147(12):4094-102.

70. Tedder T, ed. Structure of the CD20 antigen and gene of human and mouse B-cells: use of transfected cell lines to examine the Workshop panel of antibodies. Oxford University Press, 1989. (W Knapp BD, WR Gilks, et al., ed. Leukocyte typing IV. White Cell Differentiation Antigens;

71. Deans JP, Kalt L, Ledbetter JA, Schieven GL, Bolen JB, Johnson P. Association of 75/80-kDa phosphoproteins and the tyrosine kinases Lyn, Fyn, and Lck with the B cell molecule CD20. Evidence against involvement of the cytoplasmic regions of CD20. Journal of Biological Chemistry 1995;270(38):22632-8.

72. Deans JP, Robbins SM, Polyak MJ, Savage JA. Rapid redistribution of CD20 to a low density detergent-insoluble membrane compartment. J Biol Chem 1998;273(1):344-8.

73. Klasa R, O. W. Press, and B. K. Link. Monoclonal Antibody Therapy for Non-Hodgkin's Lymphoma. The Proceedings of a Symposium at the 40th Annual Meeting of the American Society of Hematology. Miami, Florida: Snell Medical Communication Inc., 1998.

74. Levine TD, Pestronk A. IgM antibody-related polyneuropathies: B-cell depletion chemotherapy using Rituximab. Neurology 1999;52(8):1701-4.

75. Shan D, Ledbetter JA, Press OW. Apoptosis of malignant human B cells by ligation of CD20 with monoclonal antibodies. Blood 1998;91(5):1644-52.

76. Tedder TF, Schlossman SF. Phosphorylation of the B1 (CD20) molecule by normal and malignant human B lymphocytes. Journal of Biological Chemistry 1988;263(20):10009-15.

77. Kuster H, Zhang L, Brini AT, et al. The gene and cDNA for the human high affinity immunoglobulin E receptor beta chain and expression of the complete human receptor

Engineering hybrid genes without the use of restriction enzymes: gene splicing by overlap extension. Journal of Biological Chemistry 1992;267(18):12782-7.

78. Adra CN, Lelias JM, Kobayashi H, et al. Cloning of the cDNA for a hematopoietic cell-specific protein related to CD20 and the beta subunit of the high-affinity IgE receptor: evidence for a family of proteins with four membrane-spanning regions. Proceedings of the National Academy of Sciences of the United States of America 1994;91(21):10178-52.

79. Tedder TF, Klejman G, Disteche CM, Adler DA, Schlossman SF, Saito H. Cloning of a complementary DNA encoding a new mouse B lymphocyte differentiation antigen, homologous to the human B1 (CD20) antigen, and localization of the gene to chromosome 19. Journal of Immunology 1988;141(12):4388-94.

80. Kinet JP, Jouvin MH, Paolini R, Numerof R, Scharenberg A. IgE receptor (Fc epsilon RI) and signal transduction. European Respiratory Journal - Supplement 1996;22:116s-118s.

81. Dombrowicz D, Lin S, Flamand V, Brini AT, Koller BH, Kinet JP. Allergy-associated FcRbeta is a molecular amplifier of IgE- and IgG- mediated in vivo responses. Immunity 1998;8(4):517-29.

82. Stamenkovic I, Seed B. Analysis of two cDNA clones encoding the B lymphocyte antigen CD20 (B1, Bp35), a type III integral membrane protein. J Exp Med 1988;167(6):1975-1980.

83. Tedder TF, Streuli M, Schlossman SF, Saito H. Isolation and structure of a cDNA encoding the B1 (CD20) cell-surface antigen of human B lymphocytes. Proc Natl Acad Sci U S A 1988;85(1):208-212.

84. Chen H, and D.A. Kendall. Artificial transmembrane segments. Requirements for stop transfer and polypeptide orientation. Journal of Biological Chemistry 1995;270:14115.

85. Denzer AJ, C.E. Nabholz, and M. Spiess. Transmembrane orientation of siganl-anchor proteins is affected by the folding state but not the size of the N-terminal domain. EMBO J. 1995;14:6311.

86. Furman I, O. Cook, J. Kasir, W. Low, and H. Rahamimoff. The putative amino-terminal signal peptide of the cloned rat brain Na^{+}-Ca^{2+} exchanger gene (RBE-1) is not mandatory for functional expression. J. Biol. Chem. 1995;270:19120.

87. Kim H, S. Paul, J. Gennity, J. Jennity, and M. Inouye. Reversible topology of a bifunctional transmembrane protein depends upon the charge balance around its transmembrane domain. Mol. Microbiol. 1994;11:819.

88. Loo TW, C. Ho, and D. M. Clarke. Expression of a functionally active human renal sodium-calcium exchanger lacking a signal sequence. J. Biol. Chem. 1995;270:16399.

89. Wong EFS, S. K. Brar, H. Sesaki, C. Yang, and C. H. Siu. Molecular cloning and characterization of DdCAD-1, a Ca^{2+}-dependent cell-cell adhesion molecule, in *Dictyostelium discoideum*. J. Biol. Chem. 1996;271:16399.

90. Polyak MJ, Tailor SH, Deans JP. Identification of a cytoplasmic region of CD20 required for its redistribution to a detergent-insoluble membrane compartment. J Immunol 1998;161(7):3242-8.

91. Kuster H, Zhang L, Brini AT, MacGlashan DWJ, Kinet J-P. The gene and cDNA for the human high affinity immunoglobulin E receptor β chain and expression of the complete human receptor. J. Biol. Chem. 1992;267:12782-12787.

92. Robbins SM, Quintrell NA, Bishop JM. Myristoylation and differential palmitoylation of the HCK protein-tyrosine kinases govern their attachment to membranes and association with caveolae. Molecular & Cellular Biology 1995;15(7):3507-15.

93. Garcia-Cardena G, Oh P, Liu J, Schnitzer JE, Sessa WC. Targeting of nitric oxide synthase to endothelial cell caveolae via palmitoylation: implications for nitric oxide signaling. Proc Natl Acad Sci U S A 1996;93(13):6448-53.

94. Dietzen DJ, Hastings WR, Lublin DM. Caveolin is palmitoylated on multiple cysteine residues. Palmitoylation is not necessary for localization of caveolin to caveolae. J Biol Chem 1995;270(12):6838-42.

95. Bubien JK, Zhou LJ, Bell PD, Frizzell RA, Tedder TF. Transfection of the CD20 cell surface molecule into ectopic cell types generates a Ca2+ conductance found constitutively in B lymphocytes. Journal of Cell Biology 1993;121(5):1121-32.

96. Stevens CF. Channel families in the brain. Nature 1987;328:198-199.

97. Olsen RW, and A. J. Tobin. Molecular biology of GABAa receptors. FASEB J. 1990;4:1469-1480.

98. Kanzaki M, Nie L, Shibata H, Kojima I. Activation of a calcium-permeable cation channel CD20 expressed in Balb/c 3T3 cells by insulin-like growth factor-I. Journal of Biological Chemistry 1997;272(8):4964-9.

99. Kanzaki M, Shibata H, Mogami H, Kojima I. Expression of calcium-permeable cation channel CD20 accelerates progression through the G1 phase in Balb/c 3T3 cells. Journal of Biological Chemistry 1995;270(22):13099-104.

100. Davidson J, J. D. Deans, and S. J. Kehl. Neither Activation of CD20 nor Depletion of Intracellular Calcium Elicit an Inward Rectifying Calcium Current in Cells Expressing CD20. Health Sciences Student Research Forum. The University of British Columbia, Vancouver, Canada, 1994.

101. Golay JT, Clark EA, Beverley PC. The CD20 (Bp35) antigen is involved in activation of B cells from the G0 to the G1 phase of the cell cycle. J Immunol 1985;135(6):3795-801.

102. Deans JP, Schieven GL, Shu GL, et al. Association of tyrosine and serine kinases with the B cell surface antigen CD20. Induction via CD20 of tyrosine phosphorylation and activation of phospholipase C-gamma 1 and PLC phospholipase C-gamma 2. Journal of Immunology 1993;151(9):4494-504.

103. Tedder TF, Streuli M, Schlossman SF, Saito H, Tedder TF, Engel P. Isolation and structure of a cDNA encoding the B1 (CD20) cell-surface antigen of human B lymphocytes

CD20: a regulator of cell-cycle progression of B lymphocytes. Proceedings of the National Academy of Sciences of the United States of America 1988;85(1):208-12.

104. Einfeld DA, Brown JP, Valentine MA, Clark EA, Ledbetter JA. Molecular cloning of the human B cell CD20 receptor predicts a hydrophobic protein with multiple transmembrane domains. Embo J 1988;7(3):711-717.

105. Tedder TF, Klejman G, Disteche CM, Adler DA, Schlossman SF, Saito H. Cloning of a complementary DNA encoding a new mouse B lymphocyte differentiation antigen, homologous to the human B1 (CD20) antigen, and localization of the gene to chromosome 19. J Immunol 1988;141(12):4388-4394.

106. Levy S, Nguyen VQ, Andria ML, Takahashi S. Structure and membrane topology of TAPA-1. Journal of Biological Chemistry 1991;266(22):14597-602.

107. Olivares L, Aragon C, Gimenez C, Zafra F. Analysis of the transmembrane topology of the glycine transporter GLYT1. J Biol Chem 1997;272(2):1211-7.

108. Kast C, Canfield V, Levenson R, Gros P. Transmembrane organization of mouse P-glycoprotein determined by epitope insertion and immunofluorescence. Journal of Biological Chemistry 1996;271(16):9240-8.

109. Dupree P, Parton RG, Raposo G, Kurzchalia TV, Simons K. Caveolae and sorting in the trans-Golgi network of epithelial cells. EMBO Journal 1993;12(4):1597-605.

110. Oettgen HC, Bayard PJ, Van Ewijk W, Nadler JM, Terhorst CP. Further biochemical studies of the human B-cell antigens B1 and B2. Hybridoma 1983;2:17-28.

111. Tedder TF, Schlossman SF. Phosphorylation of the B1 (CD20) molecule by normal and malignant human B lymphocytes. J Biol Chem 1988;263(20):10009-10015.

112. Valentine MA, Cotner T, Gaur L, Torres R, Clark EA. Expression of the human B-cell surface protein CD20: alteration by phorbol 12-myristate 13-acetate. Proc Natl Acad Sci U S A 1987;84(22):8085-8089.

113. Valentine MA, Meier KE, Rossie S, Clark EA. Phosphorylation of the CD20 phosphoprotein in resting B lymphocytes. Regulation by protein kinase C. J Biol Chem 1989;264(19):11282-11287.

114. Clark EA, Shu GL, Luescher B, et al. Activation of human B cells. Comparison of the signal transduced by IL-4 to four different competence signals. J. Immunol. 1989;143:3873-3880.

115. Snyers L, Umlauf E, Prohaska R. Oligomeric nature of the integral membrane protein stomatin. J Biol Chem 1998;273(27):17221-6.

116. Puertollano R, Alonso MA. A short peptide motif at the carboxyl terminus is required for incorporation of the integral membrane MAL protein to glycolipid- enriched membranes. J Biol Chem 1998;273(21):12740-5.

117. Cheng C, Prince LS, Snyder PM, Welsh MJ. Assembly of the epithelial Na+ channel evaluated using sucrose gradient sedimentation analysis. J Biol Chem 1998;273(35):22693-700.

118. Gold MR, Jakway JP, DeFranco AL. Involvement of a guanine-nucleotide-binding component in membrane IgM- stimulated phosphoinositide breakdown. J Immunol 1987;139(11):3604-13.

119. Chen JZ, Stall AM, Herzenberg LA. Differences in glycoprotein complexes associated with IgM and IgD on normal murine B cells potentially enable transduction of different signals. Embo J 1990;9(7):2117-24.

120. Hombach J, Tsubata T, Leclerq L, Stappert H, Reth M. Molecular components of the B-cell antigen receptor complex of the IgM class. Nature 1990;343:760-762.

121. Chang CC, Alhasan S, Rosenspire AJ. G protein mediated signal transduction: membrane immunoglobulin associated phosphoproteins identified in octyl-beta-glucoside lysates of normal B cells. Immunol Lett 1992;32(3):193-200.

122. Rubinstein E, Le Naour F, Lagaudriere-Gesbert C, Billard M, Conjeaud H, Boucheix C. CD9, CD63, CD81, and CD82 are components of a surface tetraspan network connected to HLA-DR and VLA integrins. Eur J Immunol 1996;26(11):2657-65.

123. Serru V, Le Naour F, Billard M, et al. Selective tetraspan-integrin complexes (CD81/alpha4beta1, CD151/alpha3beta1, CD151/alpha6beta1) under conditions disrupting tetraspan interactions. Biochem J 1999;340(Pt 1):103-11.

124. Horvath G, Serru V, Clay D, Billard M, Boucheix C, Rubinstein E. CD19 is linked to the integrin-associated tetraspans CD9, CD81, and CD82. J Biol Chem 1998;273(46):30537-43.

125. Kinet J-P, Alcaraz G, Leonard A, Wank S, Metzger H. Dissociation of the receptor for immunoglobulin E in mild detergents. Biochemistry 1985;24:4117-4130.

126. Mooney RA. Use of digitonin-permeabilized adipocytes for cAMP studies. Methods Enzymol 1988;159:193-202.

127. Niznik HB, Grigoriadis DE, Otsuka NY, Dumbrille-Ross A, Seeman P. The dopamine D1 receptor: partial purification of a digitonin- solubilized receptor-guanine nucleotide binding complex. Biochem Pharmacol 1986;35(17):2974-7.

128. Tedder TF, McIntyre G, Schlossman SF. Heterogeneity in the B1 (CD20) cell surface molecule expressed by human B-lymphocytes. Molecular Immunology 1988;25(12):1321-30.

129. Mole SE. Epitope mapping. Molecular Biotechnology 1994;1(3):277-87.

130. Tzartos SJ. Epitope mapping by antibody competition. Methodology and Evaluation of the validity of the technique. Methods in Molecular Biology 1996;66:55-66.

131. Jemmerson R. Epitope mapping by proteolysis of antigen-antibody complexes. Protein footprinting. Methods in Molecular Biology 1996;66:97-108.

132. Kraner S, Yang J, Barchi R. Structural inferences for the native skeletal muscle sodium channel as derived from patterns of endogenous proteolysis. J Biol Chem 1989;264(22):13273-80.

133. Zwerling SJ, Cohen SA, Barchi RL. Analysis of protease-sensitive regions in the skeletal muscle sodium channel in vitro and implications for channel tertiary structure. J Biol Chem 1991;266(7):4574-80.

134. Cohen SA, Levitt LK. Partial characterization of the rH1 sodium channel protein from rat heart using subtype-specific antibodies. Circ Res 1993;73(4):735-42.

135. Cohen SA, Barchi RL. Localization of epitopes for antibodies that differentially label sodium sodium channels in skeletal muscle surface and T-tubular membranes. J Membr Biol 1992;128(3):219-26.

136. Wang LF. Homolog scanning. Methods in Molecular Biology 1996;66:207-20.

137. Cunningham BC, Jhurani P, Ng P, Wells JA. Receptor and antibody epitopes in human growth hormone identified by homolog-scanning mutagenesis. Science 1989;243(4896):1330-6.

138. Tomlinson MG, Williams AF, Wright MD, et al. Epitope mapping of anti-rat CD53 monoclonal antibodies. Implications for the membrane orientation of the Transmembrane 4 Superfamily

Mapping the epitopes of neutralizing anti-human IL-3 monoclonal antibodies. Implications for structure-activity relationship. European Journal of Immunology 1993;23(1):136-40.

139. Morris GE. Overview. Choosing a method for epitope mapping. Methods in Molecular Biology 1996;66:1-9.

140. Tedder TF, Penta A. Structure if the CD20 antigen and gene of human and mouse B cells: Use of transfected cell lines to examine the workshop panel of antibodies. In Leukocyte Typing IV, Knapp et al., ed. Oxford University Press, Oxford, England 1989:48-50.

141. Berditchevski F, Zutter MM, Hemler ME. Characterization of novel complexes on the cell surface between integrins and proteins with 4 transmembrane domains (TM4 proteins). Mol Biol Cell 1996;7(2):193-207.

142. Tedder TF, Klejman G, Schlossman SF, Saito H. Structure of the gene encoding the human B lymphocyte differentiation antigen CD20 (B1). J Immunol 1989;142(7):2560-8.

143. Defrance T, J. P. Aubry, F. Rousset, B. Vanbervliet, J. Y. Bonnefoy, N. Aria, Y. Takebe, T. Yokota, F. Lee, K. Arai, J. De Vries and J. Banchereau. Human recombinant interleukin 4 induces Fcε receptors (CD23) on normal human B lymphocytes. Journal of Experimental Medicine 1987;165:1459.

144. Valle A, C.E., Zuber, T. Defrance, O. Djossou, M. De Rie, and J. Banchereau. Activation of human B lymphocytes through CD40 and interleukin 4. European Journal of Immunology 1989;19:1463.

145. Ilangumaran S, Arni S, van Echten-Deckert G, Borisch B, Hoessli DC. Microdomain-dependent regulation of Lck and Fyn protein-tyrosine kinases in T lymphocyte plasma membranes. Mol Biol Cell 1999;10(4):891-905.